FACULTY OF SCIENCE AND TECHNOLOGY

BACHELOR'S THESIS

Study programme / specialisation: Bygg ingeniør, Konstruksjon og Materialer	The **SPRING** semester, 2023 **OPEN** / ~~Confidential~~
Author: Khaled Habeeb	
Supervisor at UiS: Dimitrios Pavlou, PhD. Co-supervisor: External supervisor(s):	
Thesis title: **Finite Element Analysis of a Cable-Stayed Bridge**	
Credits (ECTS): 20	
Keywords: Cable-stayed Bridge, Finite Element Analysis Finite Element Method, ANSYS Workbench Meshing	Pages: 50 + appendix: 9 Stavanger, 12.06.2023

Forword

This thesis concludes the bachelor's degree in structural engineering at the University of Stavanger, Norway. The work was carried out in UiS from February to June 2023. The simulation part of the work was carried out on ANSYS Workbench software.

Sincere appreciation and gratitude to Professor Dimitrios Pavlou and senior engineer Adugna Deressa Agessa for their help and support.

Abstract

This thesis provides a static analysis of a Cable-Stayed Bridge using the Finite Element Analysis in ANSYS Workbench software.

The static loads that were taken into consideration are the traffic loads and the static wind loads on the bridge deck on longitudinal and transverse directions.The bridge chosen for this thesis is Helgeland Bridge (Helgelandbrua) in Alstahaug municipality in Nordland County, Norway.

A brief history of cable-stayed bridges and a background of construction process are presented in chapter 1, construction details are provided both for cable-stayed bridges and for the simulated bridge are included in chapter 2, details of static analysis and geometry of the bridge are then carried out in chapter 3, and small geometrical simplifications were made to achieve the best result and accuracy that the software functions allow in a way that it would not be on the expense of the accuracy of the real structure and thus the results. The calculations of the loads applied on the bridge are made according to EuroCode1. Chapter 4 is concerned with the finite element analysis, meshing process, and simulation details before leading to the results and conclusion in chapter 5. The results of the static analysis are presented both graphically and numerically and compared to the limitations of the construction materials.

A brief overview of the methodology and parts of the simulation work is presented in the Appendix with focus on the solutions for the encountered challenges. The software used for the simulation is ANSYS Workbench 2020.

Table of Contents

List of Figures and Tables

Chapter 1- Introduction

1.1 Brief history of cable-stayed bridges

The concept of supporting a beam or a pole with cables has existed for a long time. Early examples include bridges made of natural materials such as bamboo for beams and lianas, flexible long-stemmed woody vines, for ties.[1][2]

A drawing by the Croatian engineer Faustus Verantius in 1617 shown in *Figure 1.1* is an excellent illustration of how cable-stayed bridges were designed in the past, where a timber beam is supported by an I shaped bar in conjunction with suspension cables. More advanced attempts were made later in Germany in 1784 and in France in 1787, but the first confirmed bridge with inclined ties was the Kings Meadow Bridge in England in 1817 designed by two Scottish blacksmiths. Iron wires with an 8 mm diameter formed the fan-shaped stays, which are linked back into the foundations using bars with a 19 mm diameter and bolt-adjustable ties.

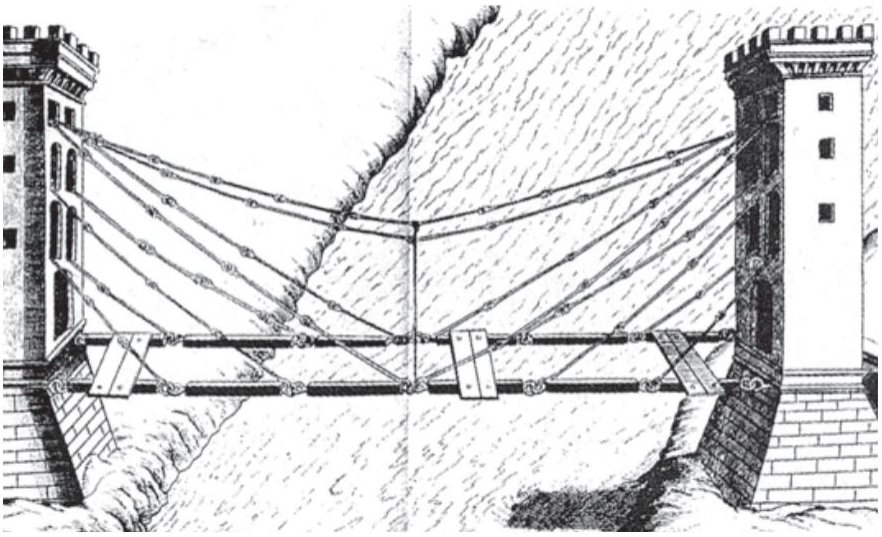

Figure 01.1 Design of ɪ shaped bar supported bridge by Faustus Verantius, 1617

In 1824, Gottfried Bandhauer designed the first German cable-stayed bridge in Nienburg across the Saale River. The bridge was exceptional in many ways; It was the longest and broadest forerunner of contemporary cable-stayed bridges and the first cable-stayed bridge to carry full road traffic, which at the time included horse-drawn carts. On the other hand, it had some flaws: the bridge was over flexible and hence susceptible to oscillations; some of the details - particularly the cable connections- lacked technical maturity, and the overall design was too

complex for the local artisans to execute. Although the collapse of this bridge and other stayed bridges led to investigations and analysis of the causes and shortcomings, it also stifled the development of this type of bridges for many years, and it did not carry on in Germany until the early 1950s. [1]

In 1851, after he immigrated to the U.S, John Roebling, a German bridge engineer, achieved a huge step forward in with the Niagara Falls bridge, *Figure 1.2*. The fundamental challenge building this suspension bridge, which has a record span of 251.5 m, was to toughen the exposed beam high above the river against severe wind oscillations and meet the required rigidity for the high train loads. He successfully accomplished these goals in two ways. In order to reinforce the beam, he first employed a 6 m deep timber truss. He then placed inclined stays in the external thirds of the main span. His greatest accomplishment however was designing the Brooklyn Bridge in New York, which set a record for span at 486 m. [1]

Figure 1.2 Niagara Falls Bridge, 1855

At least 18 transporter bridges were constructed between the late 1800s and the early 1900s, mostly around Europe. Then in 1899, the French engineer Albert Gisclard created the first tenacious and cost-effective cable-stayed bridge design shown in *Figure 1.3*. His structural system depended on inclined and horizontal cables that connect ropes to build a geometrically stable truss. The stay cables carry their horizontal components into the soil anchors through tension in the nearby cables and the second tower rather than compression in the bridge beam.

The prosperity of present cable-stayed bridges as the dominating system for large spans can be attributed to the development of high-strength steel used for the stays and advanced methods to accurately calculate the forces. The Strömsund Bridge in Sweden *Figure 1.4* that was built in 1956 is commonly regarded as the first contemporary cable-stayed steel bridge, because the concrete highway is not composite with the steel beam and simply distributes local wheel

loads. It is also categorized as a steel bridge because the concrete slab does not contribute to carrying the overall beam moments and normal forces. From a modern perspective, the completed bridge's beam has a bit too much depth being exceptionally close to the water. Apart from its non-composite highway slab, the Strömsund Bridge marks a significant advancement in the design of cable-stayed bridges.

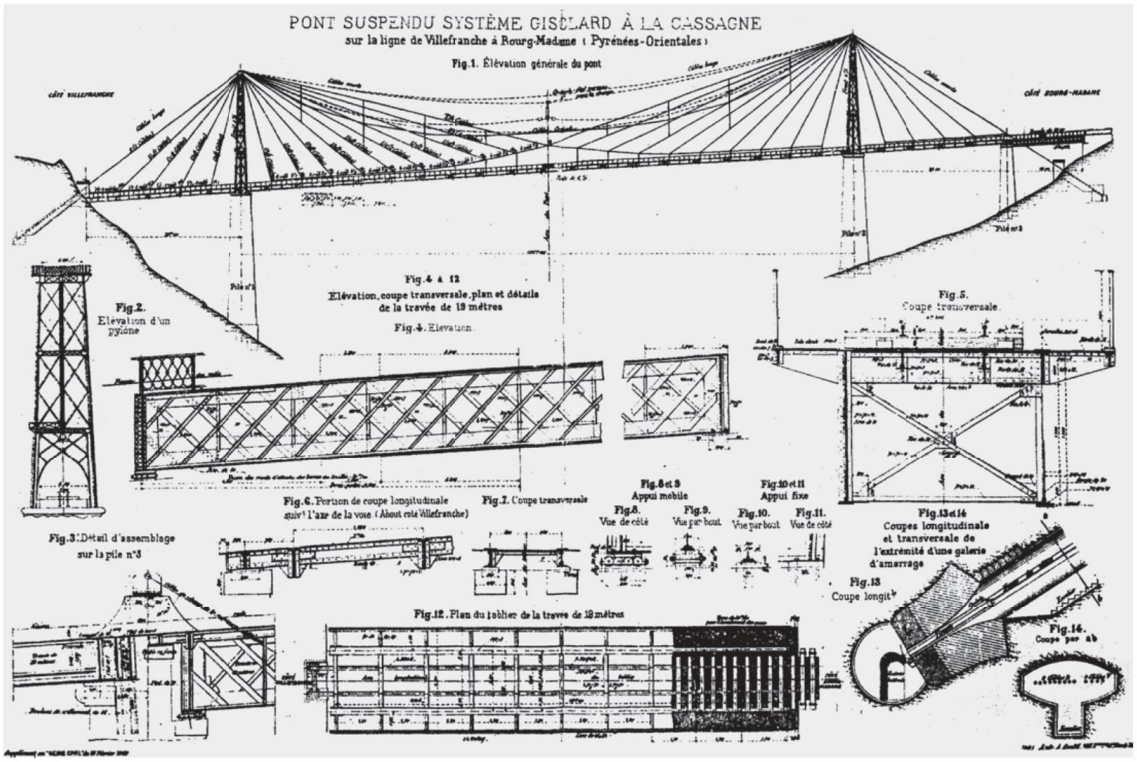

Figure 1.3 Cassagne Bridge system by Gisclard

Concrete cable-stayed bridges started to get more acceptance after the construction of Maracaibo bridge in Venezuela in 1962, with a variety of cross sections, beam thickness and stays materials where concrete stays were used instead of steel stays in some cases.

Hybrid systems bridges that have composite decks of steel and concrete became also considered due to the economic span length, where the length of the main span is a major factor for the selection of the materials as the relation between the cost per m^2 and the main span length is shown in *Figure 1.5*. [1]

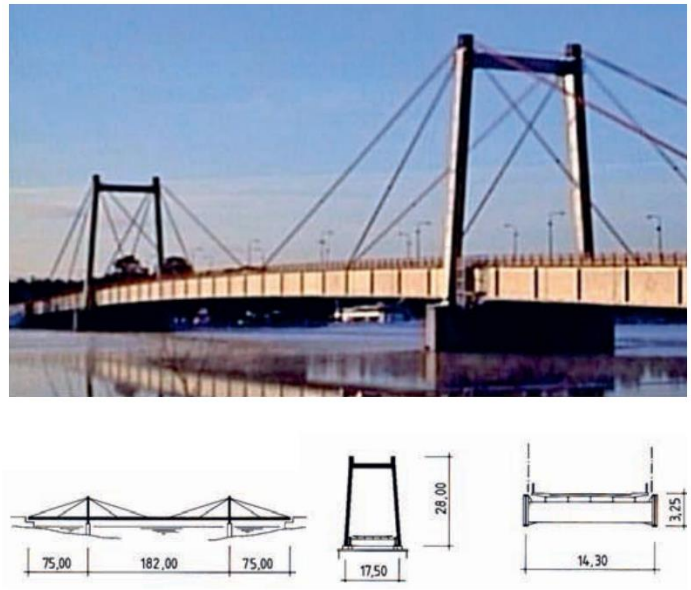

Figure 1.4 Strömsund Bridge, Sweden

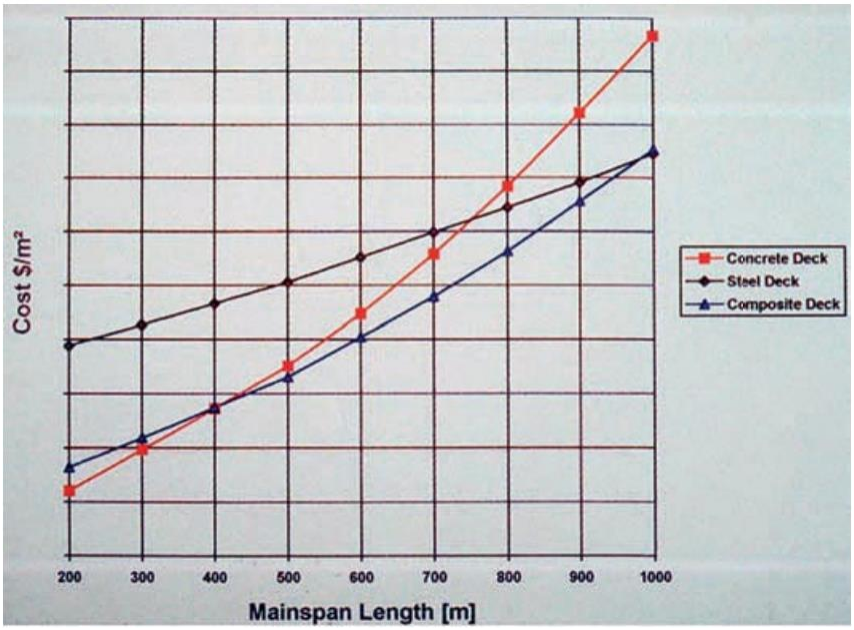

Figure 1.5 Beam cost per m2 for different types of materials

The cable-stayed bridge with the longest span is currently the Jiaxing Shaoxing Sea Bridge in China, also known as Jiashao bridge. The construction started in 2008 and was completed in 2013. Jiashao bridge is a six-pylons/towers bridge with a main span of 2680 meters, 55.6m wide and a total length of 10,138 m. [3]

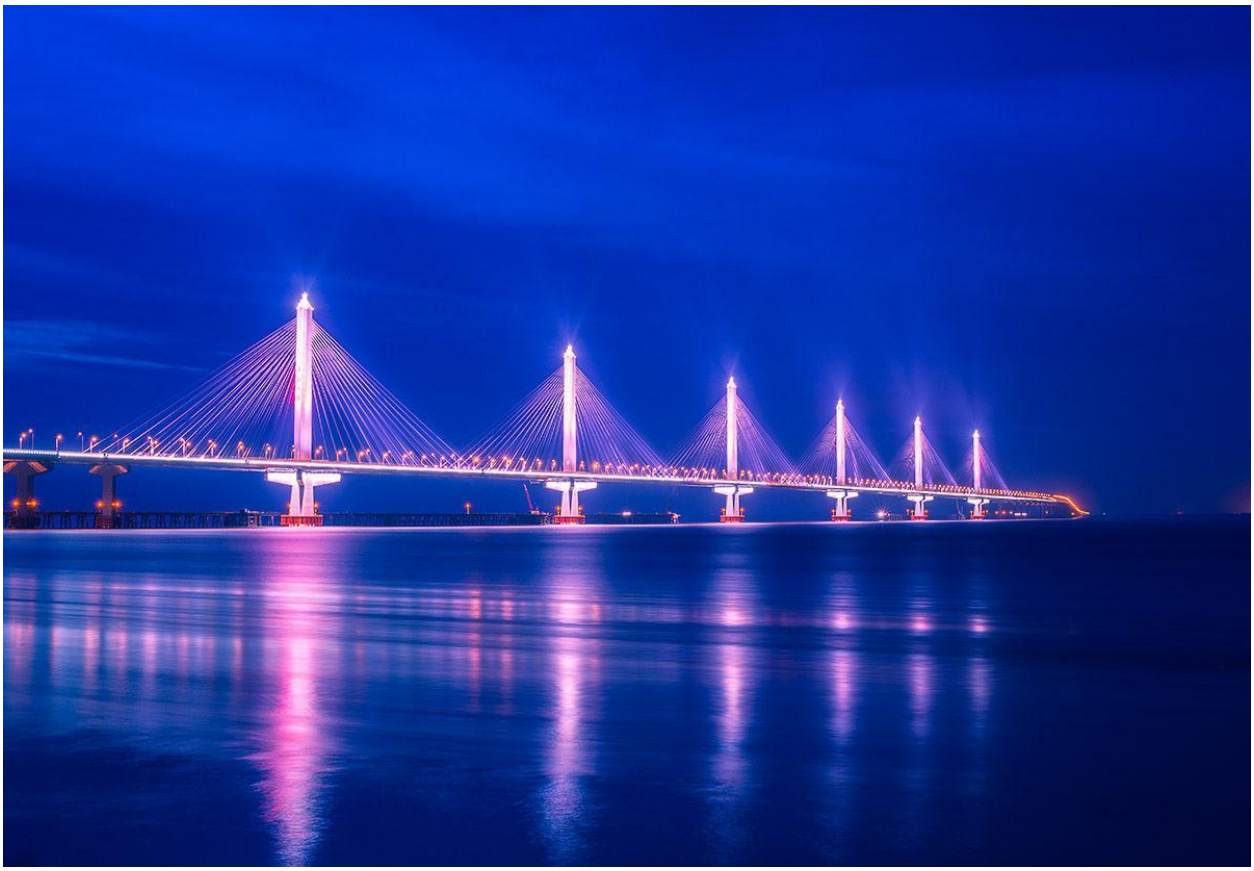

Figure 1.6 Jiashao bridge

Table 1.1 below shows the top 10 longest spans of cable-stayed bridges. [3]

No	Name	Span [m]	Girder Material	Traffic	Country	Year
1	Jiashao Bridge	2680	Steel	Road	China	2013
2	Russky Bridge	1104	Steel	Road	Russia	2012
3	Hutong Yangtze River Bridge	1092	Steel	Road & Rail	China	2020
4	Sutong Yangtze River Bridge	1088	Steel	Road	China	2008
5	Stonecutters Bridge	1018	Steel	Road	Hong Kong	2009
6	Qingshan Yangtze River Bridge	938	Steel	Road	China	2015
7	Edong Yangtze River Bridge	926	Steel	Road	China	2008
8	Jiayu Yangtzze River Bridge	920	Steel	Road	China	2019
9	Tatara Bridge	890	Steel	Road	Japan	1999
10	Normandy Bridge	856	Steel/Concrete	Road	France	1995

Table 1.1 Longest span of cable-stayed bridges

1.2 Aesthetic guidelines for cable-stayed bridge design

Even though there are no special requirements that cable-stayed bridges must meet in terms of aesthetics, they must follow the same common standards as other bridges. Yet, due to their long spans, robust constructions that can endure strong winds are needed. Therefore, the aesthetics of cable-stayed bridges must be carefully considered throughout design. It's fascinating to make comparisons with various bridge kinds.

It is generally true that there are attractive bridges that enhance the appearance of a city or a landscape and are thus enjoyed by the majority of people, and there are unsightly bridges that damage the environment to the point that many people wish they could be removed or never built to begin with. Here rises a question of what makes one bridge deemed lovely while the other is deemed hideous?

Apart from subjective aesthetic perspectives, ten standards for bridge aesthetic design are introduced and will be briefly presented. However, the flexibility of intuition and fantasy should not be constrained by these guidelines. The talent of the designer, their sensibility to aesthetics and their expertise in evaluating appearance are always prerequisites for good designs.[1]

1. Clear structural system
   A bridge must appear reliable and stable, yet the combination of various statical systems usually results in an unattractive aspect. Therefore, the variety of load-bearing components should be kept to a minimum without affecting the statically correct system that must be achieved.

2. Good proportions
   A harmonious proportion must be maintained between the structural components, the span lengths and heights, the shadowed and the luminated areas as well as the masses of the pillars, piers and the beam.

3. Good order
   Particularly for trusses, the figure and directions of the structural components should be kept to a minimum. As long as monotony does not dominate the scene, symmetry and repetition of similar elements should lead to good order.

4. Integration into the environment
   A bridge should be harmonically integrated into its surroundings, as evidenced by how well its size and materials correspond to the area around it.

5. Choice of material
   As was already discussed, choosing the right materials for aesthetics is important. It is, however, crucial to take the into account the load-bearing capacity of the materials.

6. Coloring
   Occasionally choosing an appropriate color for bridges will help them blend in with their environment. The use of vibrant colors on huge structures should be avoided.

7. Space above the bridge
   It is recommended that the area above the bridge is designed in a way that the driver can see the bridge and feel at ease while passing through it. If no bridge members rise above the bridge deck, it is helpful to make the beginning and end of a bridge visible.

8. Recognizable flow of forces
   Even a casual observer can tell instinctively if the force transfer in a bridge seems logical. A bridge's haunches should be securely supported by sturdy piers, and the pier heads should be wider than the beam's underside.

9. Lighting
   A bridge's appearance at night can be efficiently improved with aesthetic lighting. Instead of employing individual lights that simply follow the outlines, modern bridge illumination uses floodlights that cover large regions.

10. Simplicity
    The focus should be on maintaining the pure structural shape's simplicity and fineness. A single exemption should be made for any and all additions, including ornaments, decorations, and architectural features. The shape of a bridge is considered mature only if nothing can be omitted. [1]

Chapter 2- Construction background

2.1 Construction of cable-stayed bridges

The construction process of a cable-stayed bridge is obviously influenced by the size of the project, its structural system, and the local environmental factors. There are generally four different construction techniques available, two of which are most common and will be thus presented.

2.1.1 Temporary support method

The entire girder can be built on temporary supports that would be removed after the cables are added. The stiffening girder is constructed in stage one on both permanent and temporary supports. This stage allows for the application of any method used in the construction of girder bridges. In stage two, the towers from the completed girder are being erected. Afterwards, the stay cables are being installed and they need to be tensioned moderately because the optimized tensioning is controlled in the last stage.

In the fourth and latest stage, the temporary supports are removed after installing all the stay cables. The load is moved to the cable system during this procedure. The girder deflects downwards, hence in order to install the girder in the intended final position, it must be erected to a higher position. *Figure 2.1* shows the four mentioned stages.

The benefit of using this method of construction is that the girder can be built continuously from one end to the other. The process results in effective cable tension and shape management. However, the temporary supports that are used are the disadvantage. It is sometimes not economically efficient to install temporary supports, mainly when the bridge is located across a significant depth of water under the main span. [4]

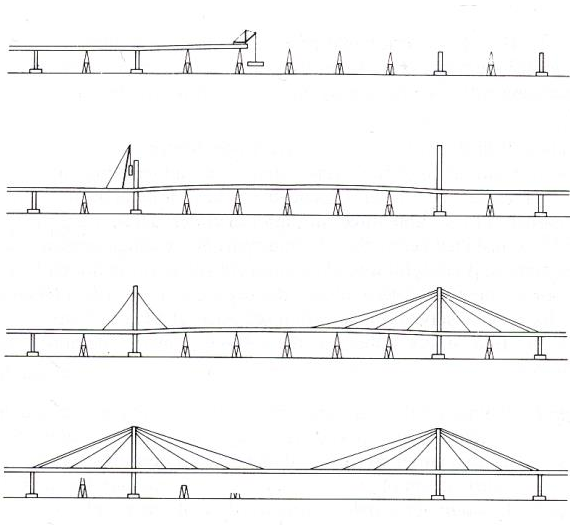

Figure 2.1 Temporary support method

2.1.2 The cantilever method

First, the towers and girder elements of the main piers are constructed. The girder pieces are then raised using derrick cranes that work from the deck area to begin a balanced free cantilever. Barges are used to convey these to the location. The stay cables are inserted and tensioned to their initial pressures to support the weight of the newly built segment as the cantilevers increase. Finally, additional loading is applied while the bridge is closed in the middle of its span.

Many constructions combine the techniques of both temporary support and cantilever methods so that the side spans are built on temporary supports and the main span is built by free cantilevering. By using this construction method, temporary supports are only applied to the side spans, where water levels or other factors are rarely an obstacle. The side spans are built first, followed by the long cantilever in the main span, which is stabilized by the already existing side, in order to take advantage of the intermediate supports in the side spans for the construction of the bridge spans. The stages are shown in *Figure 2.2*.

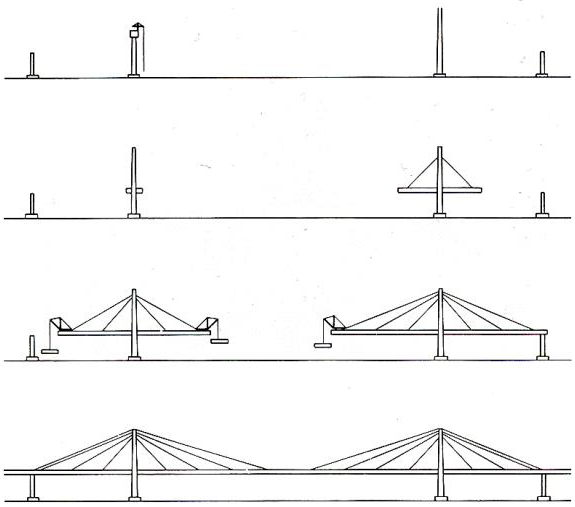

Figure 2.2 The cantilever method

The other two methods are the Rotation method and the Incremental launching method which is applied for the construction of small to medium bridges. [4]

2.1.3 Stay Cables

The stay cables transmit the forces applied to the bridge deck to the towers by being anchored to the bridge tower at one end and to the bridge deck at the other. Therefore, the integrity of cable-stayed bridges depends on the stability of the stay cables. The cables must thus have exceptional mechanical characteristics, including high tensile strength, high elastic modulus, sectional compactness, and smoothness of handling during installation. Additionally, it's essential that the cables have a good fatigue strength and excellent corrosion resistance.

Most cable-stayed bridges built between 1970 and 1985 employed parallel-wire cables, while the first cable-stayed bridges applied locked-coil cables. The locked coil rope (LCR) is made up of two types of twisted wires. Typically, round wires in the core layers and T- and Z-shaped wires in the outer layers. Smoothness and small cross sections characterize the LCR. These cables are stiffer to handle than other versions. Due to the very intricate anchoring specifics and the complexity of replacing them, these cables are rarely ever utilized today.

Parallel wire stay-cables (PWS) consist of a pack of pre-stressed wires that have a diameter of 6-7 mm placed inside a polyethylene or stainless-steel pipe that is filled with cement grout for the purpose of corrosion prevention. A steel rope is wrapped tightly around the pack to hold the parallel wires in place. In certain instances, multiple PWSs are constructed on site into one big round cable, whereas in other cases, a bundle of wires forms a hexagonal cross section.

Both steel cable-stayed bridges and prestressed concrete bridges frequently utilized these parallel wire cables. Galvanized wires and wax were later used more frequently as fillers in the pipes since they are a non-cracking and ductile substance. These cables were upgraded to the New PWS system in the 1980s.

In the New PWS cables, the protective polyethylene cover is typically extruded directly onto the wire pack eliminating any space between the wires and the surrounding pipe. The New PWS cables are more compact than conventional ones because the spiral rope and the spaces for cement grouting have been removed.

Later in the 1980s, wedge-based anchorage technology advanced parallel-strand cable (PSC) technology to increase cable protection and enhance fatigue performance. However, a technique to individually shield the parallel strands with a high-density polyethylene sheath was discovered in the 1990s. [4]

Cables are prone to physical and chemical damage even with protection coating of various materials. The chemical damage is mainly caused by environmental factors such as high amounts of salt and humidity leading to cable corrosion, since cable-stayed bridges are often constructed over water surfaces.

Corrosion of cable and coating corrosion is detected using several methods. It is extensively studied, and its distribution is modeled to accordingly use the most effective and economically efficient tools for the maintenance process and improve the longevity of the cables. [5]

2.1.4 Towers

Concrete or steel can be used to build the towers. There are several construction possibilities depending on the material and height of the structure. Mobile cranes or floating cranes can be used to install small steel towers like those seen in medium-sized cable-stayed bridges.

When casting the pylon legs for concrete towers, slip forming (continuously pouring cement into a moving form) or climbing scaffolding might be used. Because of the continuous casting, slip forming will result in shorter construction times, but it may present issues with the continuous delivery of ready-mixed concrete. Therefore, if the tower is constructed on ground where the concrete can be conveniently accessed, slip forming may be the best option. The fundamental justification for using climbing scaffoldings is the instance of the tower cast far from the coast and all the concrete needs to be brought in by sea.

When the horizontal pillar between the two legs is cast, special techniques must be used to sustain the formwork until the concrete has hardened. A transverse girder that is fastened to the tower legs is normally sufficient to achieve that.

The legs of cable-stayed bridges with diamond- or A-shaped towers are more resilient and generate significant bending moments. Therefore, it is necessary to build extra temporary struts between the two legs during construction.

The towers typically have longitudinal flexibility to follow the displacement of the cable system. The cable-stays are not in place when the tower is being built, so the tower must provide the required resistance to horizontal wind loads on its own. The most pivotal stage of the tower's construction is when it is fully erected but has no cables attached yet. Therefore, wind-induced oscillations of the tower in the longitudinal direction may occur during this stage of construction. Due to the lower mass and higher flexibility of steel structures, the wind-induced oscillation obstacle is more critical for steel towers than for concrete towers. Nowadays, it is a standard practice for large bridges to conduct wind tunnel tests to examine the stability of the free-standing towers and determine whether particular precautions are required.

Concrete towers only need a comparatively small amount of vertical reinforcement in the finished construction due to the successful pre-stressing achieved by the vertical compressive force from the cable system. The tower may therefore not have enough bending strength during construction if it is just planned for the last stage. Controlling the construction process consequently involves all structural components. [4]

2.1.5 Bridge deck

When cast-in-place decks are under construction, a mobile carriage supports the weight of the new section of the fresh concrete using longitudinal beams or frames that extend into the cantilever from the previous section.

Another possibility is utilizing a cable-stayed mobile carriage for the construction of the main concrete girder. There are two methods that could be used: The initial step is to stabilize the mobile carriage in each of its subsequent places using temporary cables. The second is to use final cables, which are later anchored to the concreted section, to maintain the movable carriage in the erection position.

For cable-stayed bridges, cast-in-place constructions are advantageous because they permit some limited tensile stresses during assembly. When the final construction is in its perfect state, the bridge is then in an excellent position to handle a designed amount of live load without creating any tensile stress in the concrete components. Members made of partially prestressed concrete can then balance extreme live loads. Precast segments cannot be used for partial pre-stressing since they might be chosen in bridges with significant inertia.

Steel girders and concrete decks work together in composite cable-stayed bridges to provide stiffness and resistance to applied bending and axial forces on the structure. The structure is clearly lighter than concrete decks due to the use of steel. In terms of a pure steel deck, the

steel components are prefabricated with excellent quality control and precise dimensions. The concrete deck, which also takes the majority of the axial stress of the cables, is what creates the roadway, which is typically covered in an asphalt or concrete overlay for traffic wear. [4]

2.2 CIP concrete cable-stayed bridges - Helgeland Bridge

Helgeland Bridge is located in the west cost of Norway, northeast of the town of Sandnessjøen in Alstahaug municipality in Nordland County. The bridge crosses the Leirfjord connecting the island of Alsten to the mainland. *Figure 2.3* shows the local view of the positioning of the bridge, and *Figure 2.4* shows the national view of the positioning.

Figure 2.3 Local view of the position of Helgeland bridge

Helgeland Bridge is a slender cable-stayed CIP (Cast in Place) concrete bridge. Its main span is 425m long, with two side spans of 177,5m each, yielding a full span of 780m long. The aerodynamically shaped beam has a 12m width and 1,2m depth, and the two towers are founded on rocks 30m deep. Bridge layout is shown in *Figure 2.5*.

The main advantage of CIP concrete that the bridge beam was built with is that there is no need to lift and move heavy precast elements. On the other hand, the disadvantage of CIP concrete

construction is that it entails one to two weeks for each beam segment to be constructed, compared to one to two segments per week that precast elements allow. This means that CIP constructions take on average double the time of precast elements constructions. To speed up the construction, long beam parts of 12m were utilized.

Figure 2.4 National view of the position of Helgeland bridge

The geology around the bridge is composed of granite rocks that have been partially gouged by glaciers from the ice age. The fjord is over 400 meters broad and reaches 130 meters deep and has steep slopes on all sides. At first, a 400m main span was proposed, but it had to be extended to 425m to appropriately remove the foundations of the towers from the edges of the fjord for the purpose of properly preventing the granite slopes from sliding.

Due to the limited volume of traffic at this site, only two traffic lanes and one walkway were required, resulting in a 12 m wide beam. Regular B65 high-strength concrete was used throughout the construction. [1]

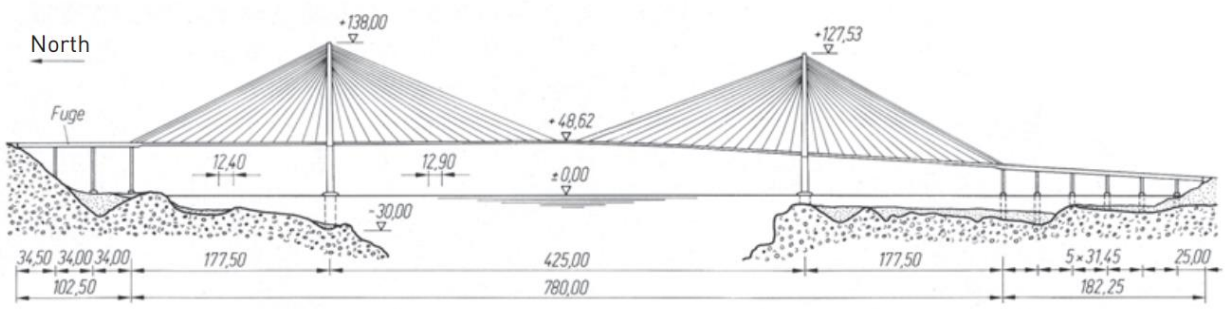

Figure 2.5 Bridge layout

Cross girders are situated at the points of cable anchoring, distancing 12,9 m. The roadway slab extends 12,4 m longitudinally and 7,5 m transversely with a thickness of 0,4 m. The loads during construction, live loads, permanent loads, and turbulent winds are the regulating loads for choosing the size of the beam. The bridge cross section is shown in *Figure 2.6* below.

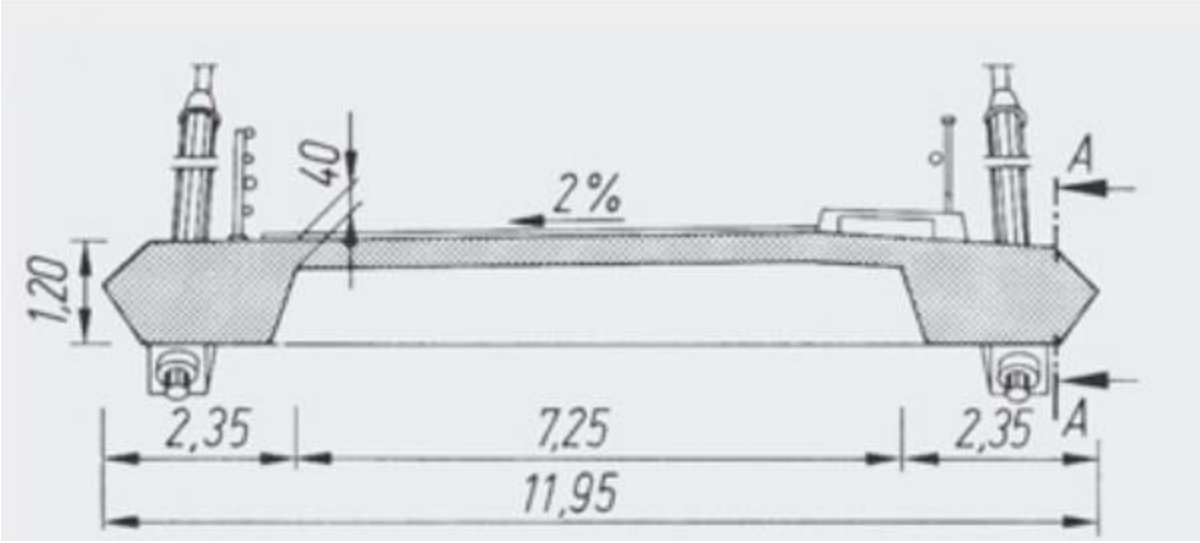

Figure 2.6 Bridge cross section

Diamon shaped towers were selected due to economic and aesthetic criteria, in addition to its developed torsional resistance of the beam.

Figure 2.8 shows the North tower, which is 10,5 m higher than the south tower as it could be seen in *Figure 2.5*.

The stay cables were sized according to PTI (Post-Tensioning Institute) criteria for galvanized wires, at 7 mm radius and 1450/1650 steel.

Four sets of 32 stay cables (total of 128 cables) with lengths varying from 64 to 225 meters demanded 67 to 231 wires that are also covered with PE (Polyethylene) pipes. [1]

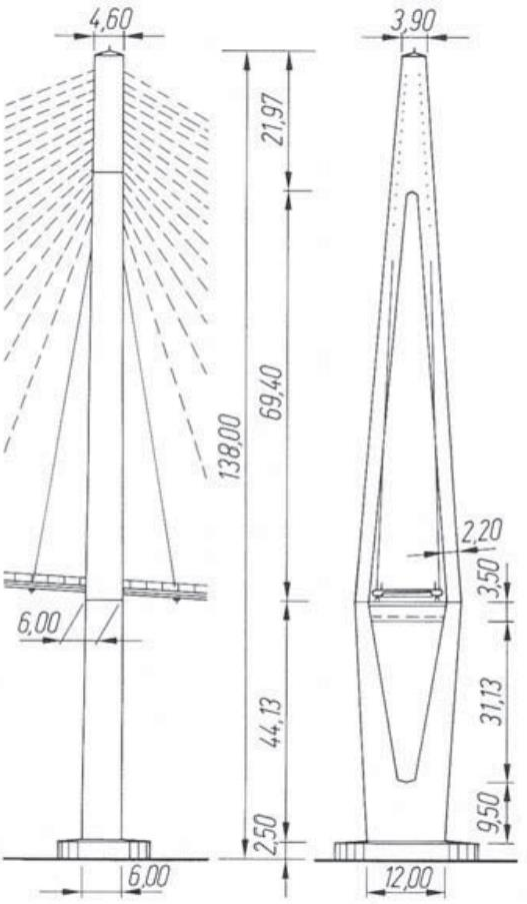

Figure 2.8 North tower

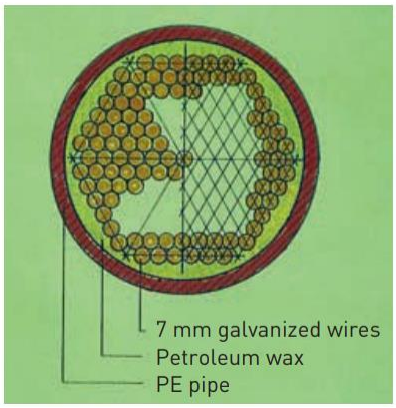

Figure 2.7 Cable cross section

50 years probability, final stage		
Wind speed	Height +10m	Height +50m
10 min. mean	40 m/s	50 m/s
Gust (3-5 seconds)	60 m/s	70 m/s

Table 2.1 Wind characteristics

The Gulf Stream mitigates extremely low temperatures in this area, but a real challenge is the recurrent severe storms. A careful and detailed analysis of the wind response was therefore required, both during construction and for the final structure, due to exposure of the location to high wind speeds. Wind characteristics based on measurements taken over 50 years are presented in *Table 2.1* above.

Aerodynamic instabilities were shown to be unlikely by wind tunnel studies on elastically supported, dynamic section models. The testing using a complete model in a boundary layer wind tunnel revealed, as usual, that turbulent wind has the biggest amplitudes. The thorough aerodynamic analysis demonstrated adequate safety for both the final stage and the construction phase. Despite the fact that the projected strong storms having a 50-year probability did in fact happen, the bridge was stable while it was being built. A good correlation between the predicted and observed deformations was evident in the control measurements.[1]

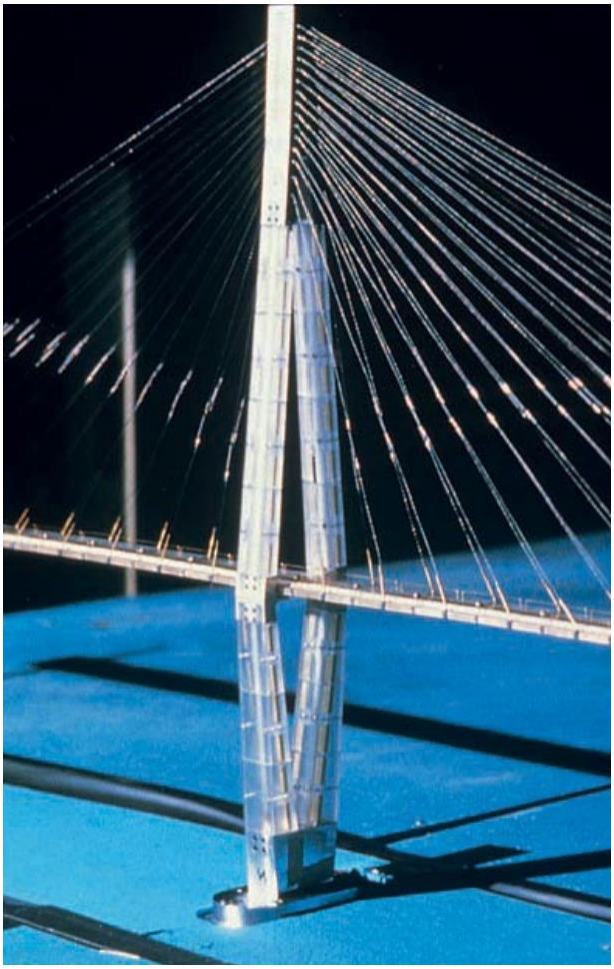

Figure 2.9 Full model for boundary layer wind tunnel test

The project was granted by Statens Vegvesen Norway in 1989 to Aker Entrepreneur, a Norwegian contractor. With collaboration of subcontractors in Germany for the towers,

Switzerland for the stay cables and Canada for the wind tunnel tests, the bridge was opened on June 21st, 1991. [1]

Figure 2.10 Helgeland bridge from two different points of view

2.3 Construction and climate

Due to the position of the bridge northwest of Norway and close to the Arctic Circle, challenging weather conditions had to be taken into consideration for the construction planning. The issue was violent storms that frequently happen throughout the winter months, not low temperatures, which were avoided by the Gulf Stream's effect. A risky undertaking was the free cantilevering for 210 m from each tower with a beam depth of only 1.2 m. During free cantilevering storms with winds up to 70 m/s (252 km/h) threw the spray up to beam level.

In order to prevent segregation during batching, a specific mix of concrete was created for the tower foundations, which were constructed 30 meters under the surface. Beginning with the application of a primary layer of concrete by divers on the ready-made rock surface, foundation building began.

The precast components for the underwater sections were cast onshore and floated to the location. A floating crane was used to lower the precast components onto the ready foundation where they were then underwater stressed together and filled with CIP concrete.

The essential design of the beam took into consideration that the construction would be carried out for CIP concrete by free cantilevering from the towers outward to both sides in portions of 12.90 m, which is equal to the cable distances. Additionally, it was intended during the design process to use permanent stay wires to support the travelers as shown in *Figure 2.11*.

Figure 2.11 Elevation of the traveler

The cables were shipped from its manufacturing facility in Zurich, Switzerland, to the construction location and then raised to the beam. Each cable anchor was then raised to the

tower head by the tower crane, threaded into the steel pipe, and anchored there. Some of the leading cables oscillated while free cantilevering in the face of high winds, with amplitudes the size of several cable diameters. This phenomenon is well-known from building other bridges and it is essentially due to the flexible beam tips during free cantilevering and the significant sag of the stay cables caused by missing beam loads are the causes, both of which promote wind oscillations. These could result in significant cable amplitudes from what is known as anchoring excitation.

Hydraulic and friction dampers were examined as a means of reducing these cable oscillations. However, in order to minimize slackening and make maintenance simpler, 4x3 tie-down strands of stainless steel with 15 mm in diameter per cable plane were placed. The disadvantage with these tie-downs is that they obstruct the aesthetics of the bridge and make it challenging to inspect the cables while carriages are moving along them. [1]

Figure 2.12 Stay cables tie-downs

2.4 Wind Tunnel Studies

Currently, wind tunnel section model experiments are the major method used to derive the fundamental aerodynamic parameters or functions, such as force coefficients, flutter derivatives, and aerodynamic admittance functions, are needed for wind-induced response assessments of long-span cable-supported bridges.

Full aeroelastic model studies are frequently performed in wind tunnels to monitor and measure the aeroelastic behavior of long-span cable-supported bridges in order to assure their functionality and safety under high wind conditions. In order to investigate novel aerodynamic or aeroelastic phenomena, such as rain-induced cable vibration, wind tunnel investigations are also carried out. Additionally, there are numerous circumstances in which it is impossible to anticipate the wind load and the effects it will have on bridges and vehicles with enough accuracy, either to ensure functionality and safety or to avoid adding excessively expensive safety features. In these circumstances, testing structural models in a wind tunnel can be advantageous.

The development of numerous huge wind tunnels that produce turbulent boundary layer models of the actual wind has led to significant advancements in modeling methods for wind effects on bridge constructions. The measurement precision has been greatly increased by the development of new measurement methods employed in wind tunnel experiments.

To collect wind-effect data exemplary of real-world conditions, a boundary-layer wind tunnel needs to be able to generate flows that mimic the essential features of natural wind at a location. Furthermore, it must have a test section that is long enough to create a thick vertical boundary layer, tall enough to prevent the boundary layer from touching the tunnel ceiling, and wide enough to include nearby buildings and topographical features in the model. Additionally, the blockage ratio (defined as the difference between the cross-sectional areas of the model blocking the flow and the cross-sectional areas of the tunnel test section) must be less than or equal to about one-twentieth.

In addition to installing roughness components on the tunnel floor, upstream additions like spires must also be put in place in order to promote the quick establishment of a vertical boundary layer along the tunnel test section. A similar velocity profile and kind of turbulence to those experienced by the prototype structure must be produced by the roughness and the spires.

The model being tested in a wind tunnel is normally mounted on a turntable so that it may be examined for winds coming from various directions. The model should include the specific structure to be tested as well as other nearby structures and terrain elements, all built to the same scale ratio, in order to accurately recreate the wind field.

The cross-sectional area of a tunnel test section must be expanded to a certain degree in the direction of the wind to maintain constant pressure (zero gradient of pressure) through the whole tunnel. In order to make up for the pressure loss brought on by friction, the increased cross-section produces a drop in wind speed and an increase in pressure in the wind direction. Typically, the tunnel test section's adjustable ceiling is used to enhance the space. A zero-pressure gradient in the wind direction is created by adjusting the ceiling slope. [6]

Figure 2.13 shows the components of boundary-layer wind tunnel test section.

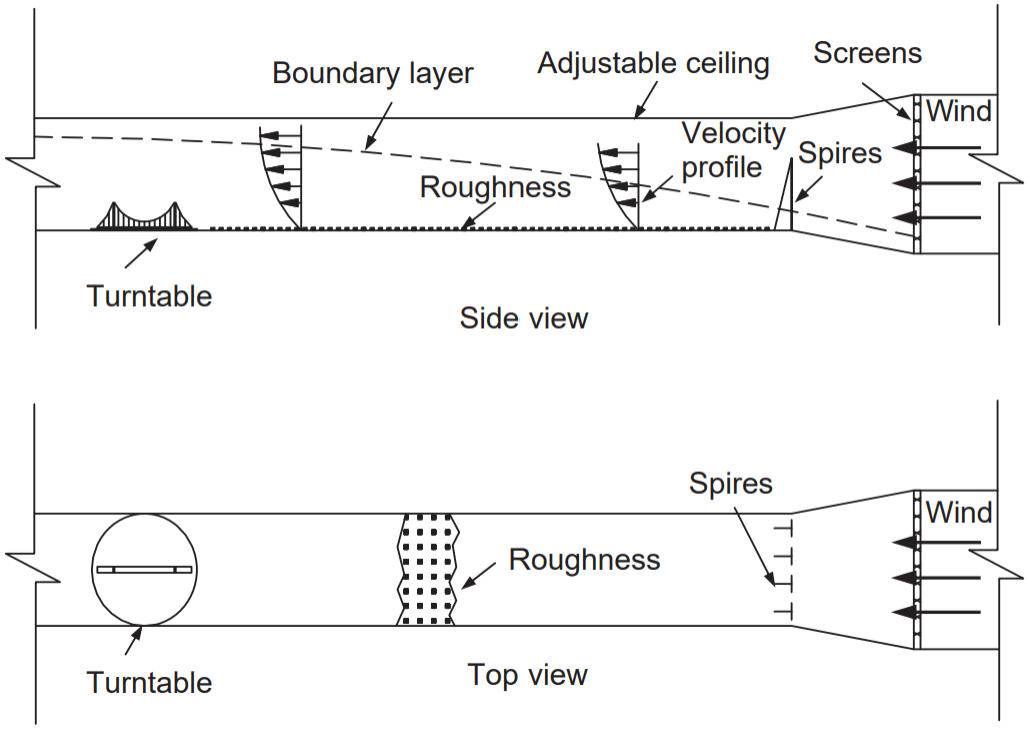

Figure 2.13 Components of boundary-layer wind tunnel test section

Chapter 3- Geometry and Static Analysis

3.1 Geometrical simplifications

As with any engineering project, a sketch of geometry is essential to move to the designing and later simulation part of the project. In this thesis, the sketching was carried out in ANSYS Workbench environment, and an approach of simplification was done to adapt to the purpose of this thesis.

3.1.1 The positioning of the bridge

The incline and asymmetry in the main span of the bridge was simplified to be modeled as a fully horizontal bridge. Since the wind loads on the towers and on the Z axis for the bridge are not calculated, this simplification would have no effect on the results. In addition, this was a necessary adjustment of the geometry in order to make use of the functions that the software offers such as creating pattern and mirroring.

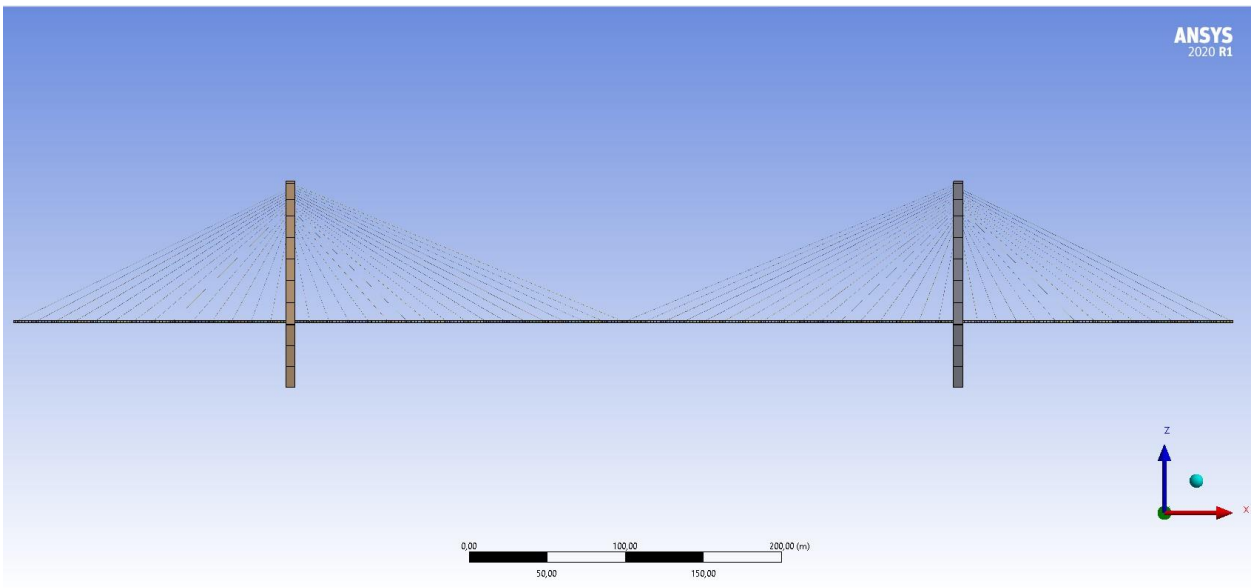

Figure 3.1 Side view of the simulated bridge

3.1.2 The bridge deck

The length of the full span and main span were kept precise and unaltered. However, simplifying the spacing between the girders of the bridge body was necessary due to pattern function complications in the ANSYS software, in addition this simplification is of a minor effect when studying the live (traffic) loads and the wind loads. The spacings between the girders in the original bridge is 12,9 m in the main span and 12,6 in the side spans. The one simulated in ANSYS was taken at 12,58 m.

However, simplifying the shape of the cross section of the bridge was necessary due to the pattern function in ANSYS. The result was not of a negligible difference and the final form of the bridge deck is shown in *Figure 3.2* below.

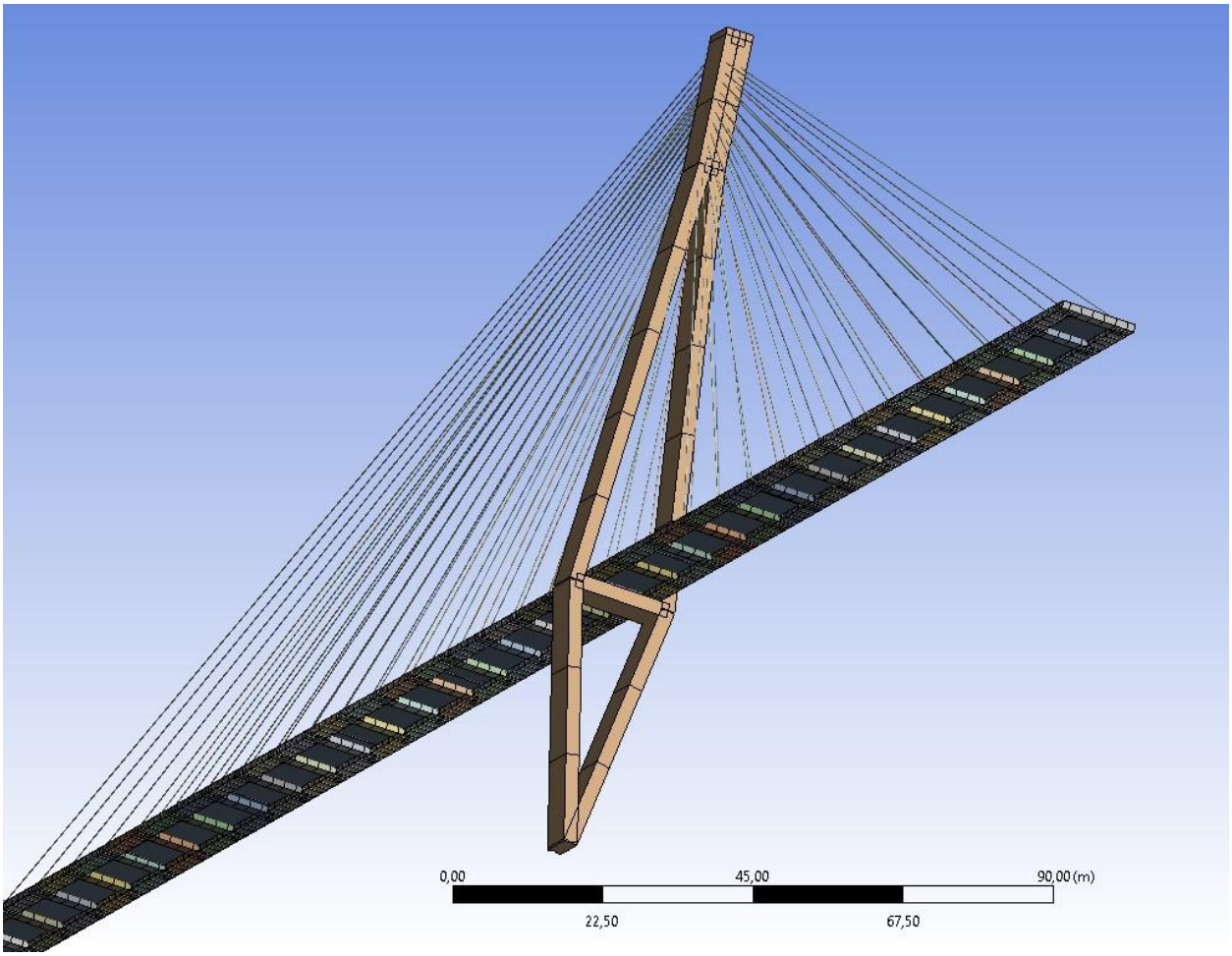

Figure 3.2 Simulated bridge deck from below

The dimensions of the bridge plate were not modified. It has a depth of 0,4 m and a width of 7,5m. However, it was sketched and simulated as one piece of concrete (one element in the software).

3.1.3 Cables

As the spacing between the girders was modified as mentioned above, and the spacing of cables followed the same pattern, i.e., the cables were connected to the bridge beam at the same connection points of the girders.

The spacing of the cables on the towers was also simplified to 1,5 meters vertically, starting with two points on the inclined part of the towers and then proceeding with the rest on the vertical part.

The total number of connection points on each tower is 34 points, 17 on each side of the tower, and they were used for connecting the cables from both sides. The distribution of the cables from each tower is 28 cables towards the side span (14 to each side of the bridge beam) and 34 cables towards the main span (17 to each side of the bridge beam), with a total of 124 cables.

The calculation for the cables cross section is carried out later in section 3.3 and applied accordingly in the software.

3.1.4 Towers

Simplifying the shape of the towers was done basically since the wind loads on the towers are dynamic loads and hence not taken into consideration for the purpose of this thesis. Therefore, the exact shape for them is of a negligible effect. Also, the cross section of the towers was simplified to be of a unified form from top to bottom with dimensions. This yielded having a cross section of 2,2x6 m.

The towers are placed $((14\ plate * 12{,}58\ m = 176{,}12\ m))$ from each of the ends of the bridge. That is only a 1,38m deviation from the actual distance for the real bridge.

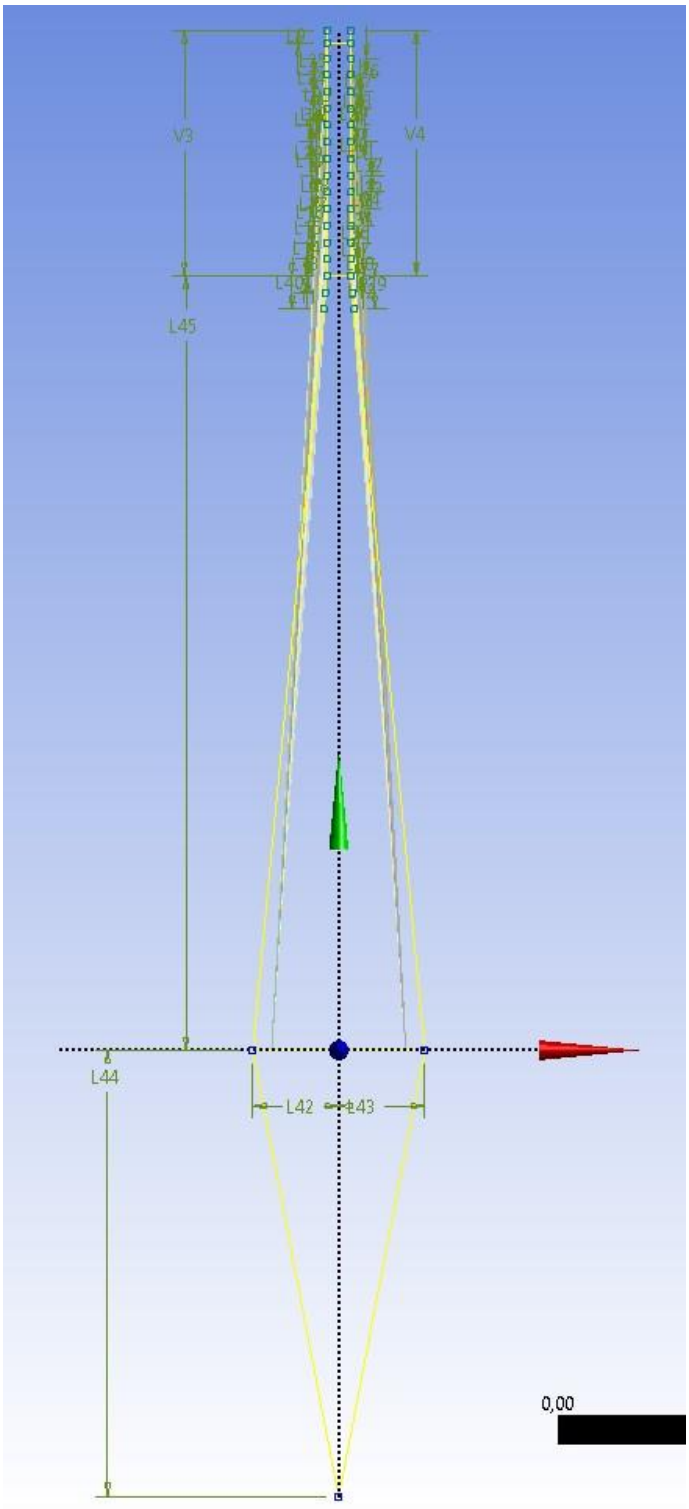

Figure 3.3 Cables connection points on the tower

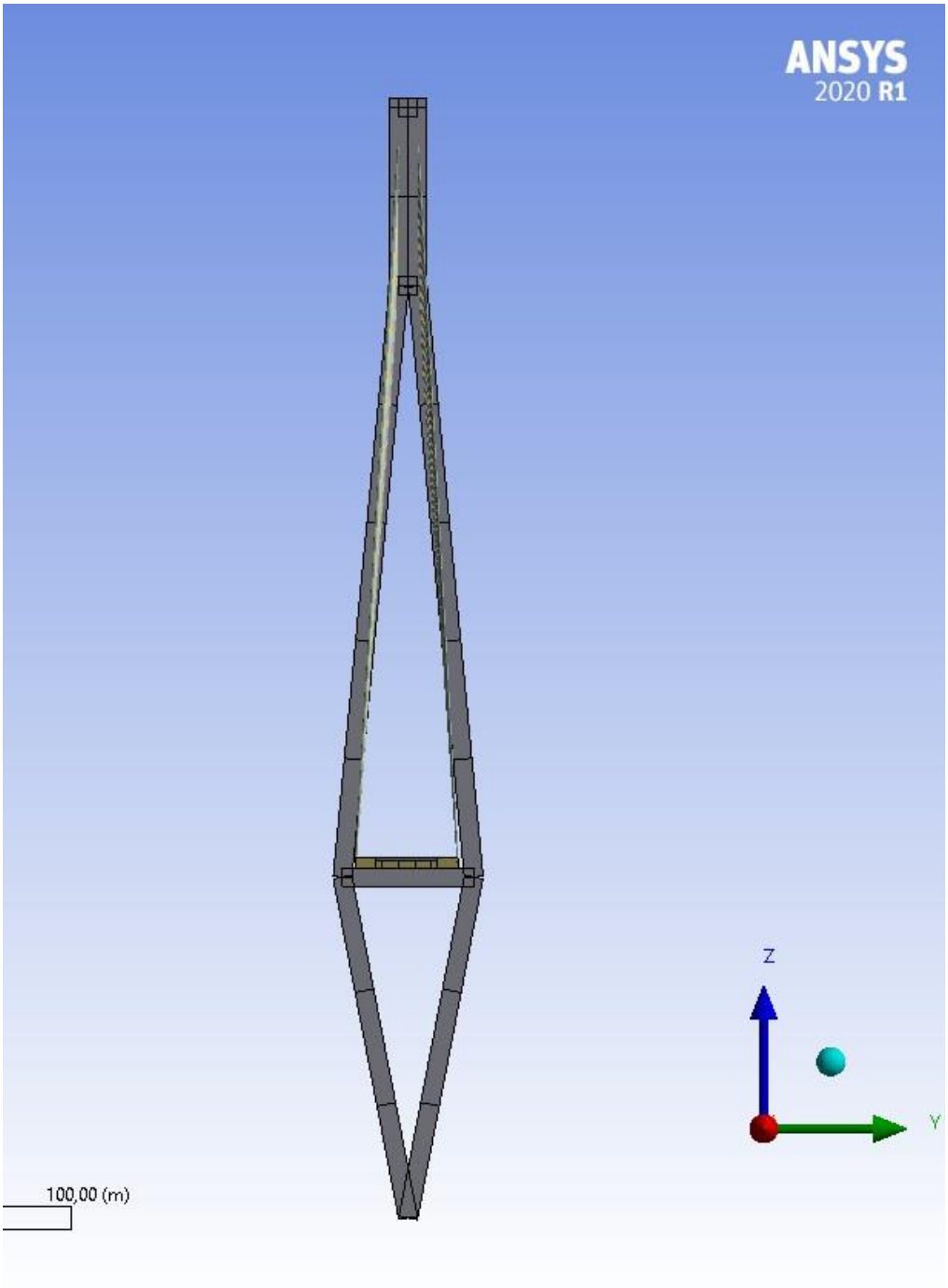

Figure 3.4 Front view of the bridge after meshing

The final overall geometry of the bridge is shown in *Figure 3.5* and *Figure 3.6* illustrates the final overview of the geometric sketch before and after the meshing process.

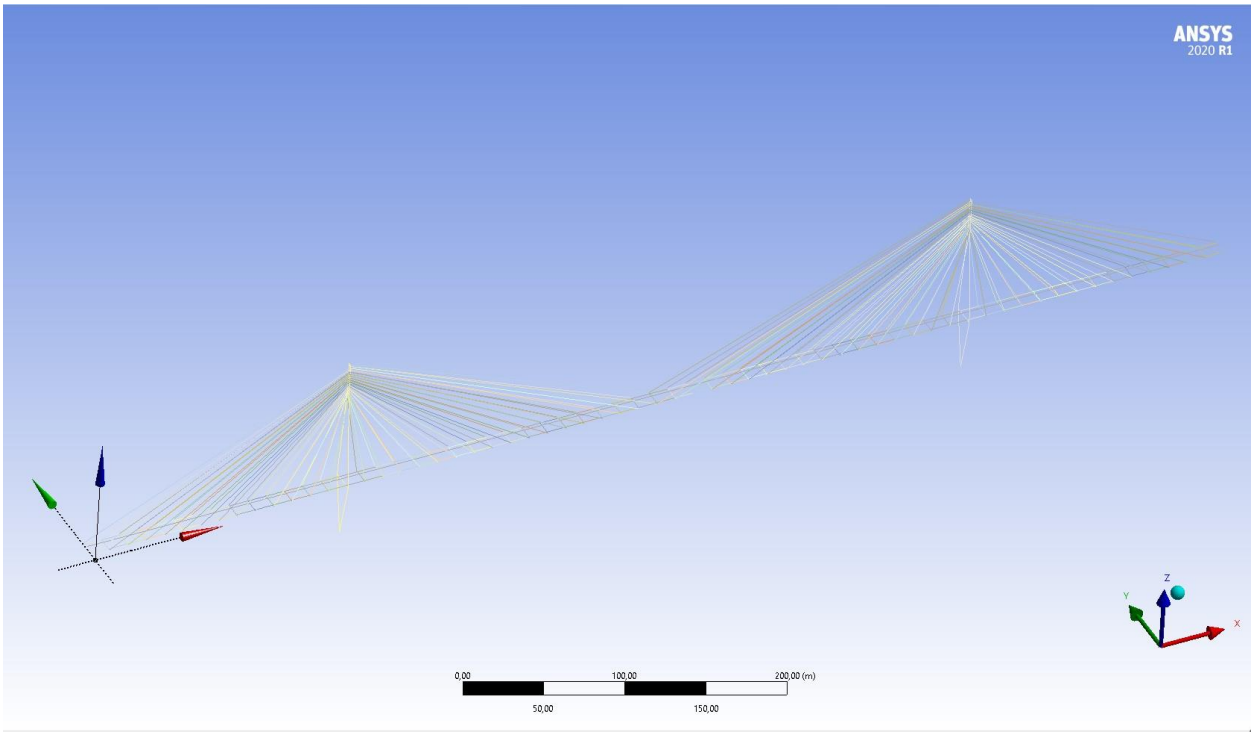

Figure 3.5 The final geometric sketch of the bridge

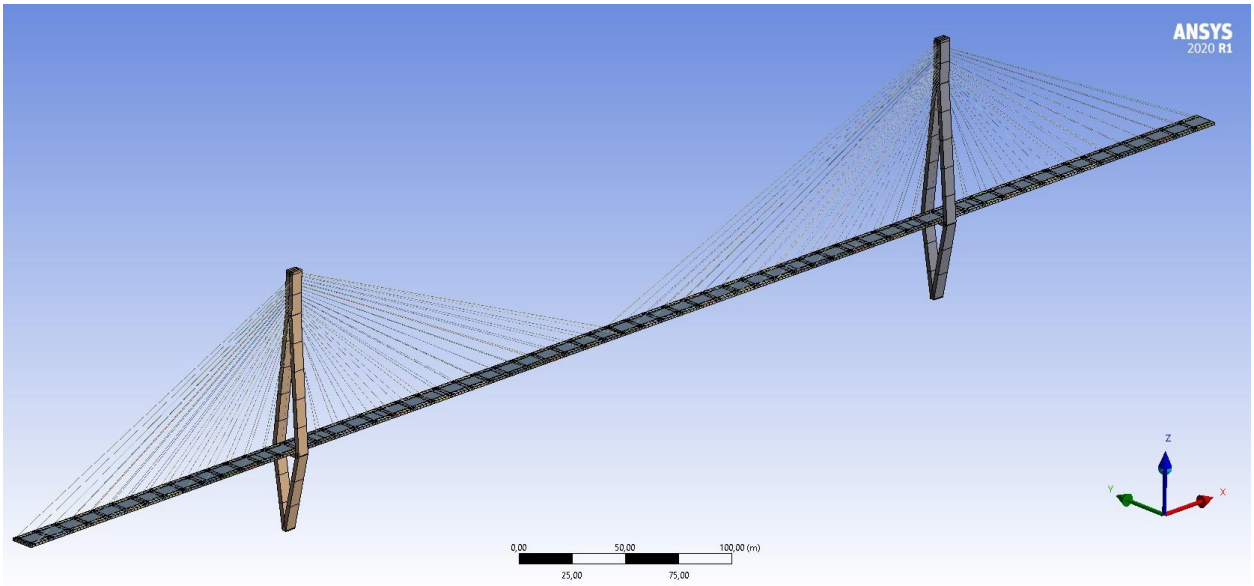

Figure 3.6 The bridge after meshing

3.2 Static Analysis

The following sections will describe the loads applied on the simulated structure.

3.2.1 Live loads

Live loads might differ in size and location. They might be brought on by forces of nature, moving vehicles, or weights of objects that have been momentarily put on a structure. The minimum live loads required by codes are established through an analysis of their historical effects on existing structures. These loads typically feature additional safeguards against excessive deflection or unexpected overload.

Traffic-related live loads make up the majority of loads on bridge spans, and a convoy of trucks is the source of the heaviest vehicle loading. There are standards in each country with specifications that list the dimensions of the "standard truck" and the weight distribution. Even if vehicles are supposed to be on the road, the bridge does not need to be completely filled with a row of trucks in order to achieve the critical load because such a loading is extremely unlikely. However, considering that live loads behave like dynamic loads due to the variation of the loads resulted from the different axles of the truck and their movement, the traffic-related live loads in this project would be treated as static loads for a bridge fully stacked with trucks, and the calculations carried out in next section. [7]

3.2.2 Wind loads

The infamous collapse of the early Tacoma Narrows Bridge back in 1940 determined the importance of comprehending the wind effects on long-span cable-supported bridges, a category includes cable-stayed and suspension bridges. Thanks to the substantial research and practice that have been done since then, and the developments have been made mainly in the past 40 years, it has been possible to build suspension bridges with a main span over 1990 m and cable-stayed bridges with a main span over 1000 m.

In this century, it has become increasingly clear that super-long-span cable-supported bridges are required to traverse straits and to connect people and enhance their life. However, the large increase in damaging windstorms brought on by climate change has had an impact on many regions of the world, making long-span cable-supported bridges significantly more susceptible to severe winds. Hence the imperative need for thorough and comprehensive wind load assessment and analysis.[8]

As mentioned in section 2.4, current wind loads data are mainly harvested by wind tunnel tests. However, the calculations made for this project are carried out according to EuroCode1 that recommends the simplified method when the structure is assessed to not be responding dynamically to the changing wind load. This is ideal for the purpose of this project, i.e., static analysis.

The analysis of wind load is performed only on the bridge deck, and even though the effect of the wind loads act in three directions; where X is transverse, Y is parallel and Z is perpendicular to the deck, only X and Y directions are considered.

Force in X (transverse) direction is also known as drag force, and it is given by the equation:[9]

$$F_w = \frac{1}{2} * \rho * V_b^2 * C * A_{ref,x}$$

Where:

V_b	is the basic wind speed.
ρ	is air density.
C	is the wind load factor.
$A_{ref,x}$	is the reference area.

For force in Y (longitudinal) direction, the approximated value is 25% of the force in X direction for plated bridges, i.e., bridges with box girders or solid plate girders, and 50 % for trussed bridges.

3.3 Calculations

After the clarifications of the geometrical simplifications, the calculations done in order to input data in ANSYS are presented in the next three subsections.

3.3.1 Wind loads

Force in x direction is calculated by equation:

$$F_w = \frac{1}{2} * \rho * V_b^2 * C * A_{ref,x}$$

Sub calculations for $A_{ref,x}$ includes:

$$A_{ref,x} = d_{tot} * L$$

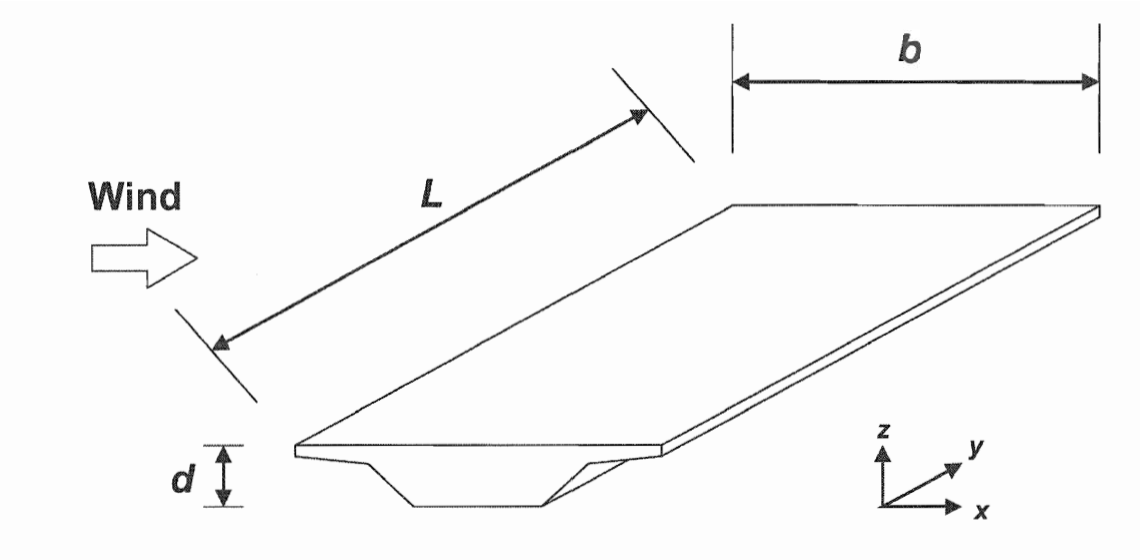

Figure 3.7 Directions of wind actions on bridge

For an open parapet with an open safety barrier:

$$d_{tot} = d + 0{,}3$$

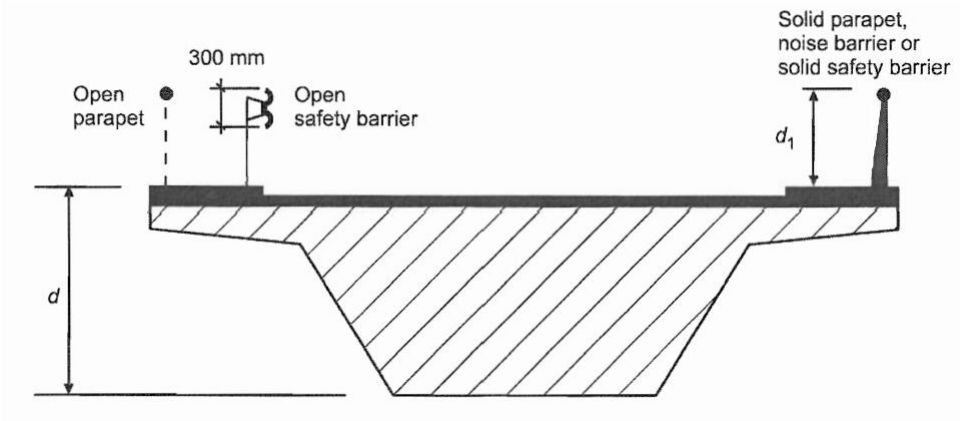

Figure 3.8 Depth to be used for A_(ref,x)

Sub calculations for C relies on recommended values of C that are given in the following table.

b/d_{tot}	$Z_e \leq 20m$	$Z_e = 50m$
≤ 0,5	6,7	8,3
≥ 4	3,6	4,5

Table 3.1 Recommended values for C

For the Helgeland bridge:

d=1,2m b=12m Z_e = 45m

Putting all the values in the equation and calculating for a mean wind speed on heights +50 m:

$$F_w = 0{,}5 * \left[1{,}239 \frac{kg}{m^3}\right] * \left[50^2 \frac{m^2}{s^2}\right] * 4{,}5 * [1{,}5m] * [780m] = 8154\ kN$$

Applying the wind load in ANSYS as a line pressure, dividing on the length:

$$\frac{8154\ kN}{780\ m} = 10{,}454\ \frac{kN}{m}$$

Force in Y direction (longitudinal direction)

Since Helgeland bridge is a plated bridge, the approximated value is 25% of the force in X-direction. This gives:

$$F_{w,y} = 0{,}25 * 8154\ kN = 2038{,}5\ kN$$

Also applying it as a line pressure in ANSYS, dividing on the width:

$$\frac{2038\ ,5\ kN}{12\ m} = 169{,}9\ \frac{kN}{m}$$

3.3.2 Live loads

The bridge was designed according to the Norwegian codes which require a 600 kN truck for live loads in addition to a Uniformly Distributed Load UDL of 3kN /m2. [1]

Calculating UDL for the whole bridge:

$$\left[3\frac{kN}{m^2}\right] * [780m] * [12m] = 28080\ kN$$

Calculating for a line pressure value to input in ANSYS:

$$\frac{28080\ kN}{780m} = \ 36\frac{kN}{m}$$

While the live load is considered a dynamic load [7], it could be approximately calculated by assuming a bridge full of 600 kN trucks even though the traffic on this specific bridge is quite light [1]. According to International Transport Forum, the "European Modular System (EMS) combinations may have a maximum length of 25.25 m and maximum weight of 60 t on a designated road network." Comparing with 600kN from the Norwegian standards and the maximum length of lorries, the load on a two-lanes bridge full of lorries can be calculated as follows:[10][11][12]

There are 62 parts(plates) of 12,58 m length in the two-lanes simulated bridge, considering that each lorry occupies 2 plates that yields:

$$62 * 600kN = 37200kN$$

Calculating to apply the load as line pressure in ANSYS:

$$\frac{[37200kN]}{780\ m} = 47{,}692\ \frac{kN}{m}$$

Thus, the total load on the bridge is calculated as the sum of:

$$36\frac{kN}{m} + 47{,}692\frac{kN}{m} = 83{,}692\frac{kN}{m}$$

3.3.3 Calculation of the cross section of the cables

The isolation materials are not taken into consideration when calculating the cross section of the cables, it is only the steel wires that are the actual element that should be modeled. Taking the maximum number of wires included in one cable and calculating.

$$231 * 0{,}007^2 * \pi = 0{,}0355\ m^2$$

Calculating r to input the cross section into ANSYS:

$$\pi * r^2 = 0{,}0355\ \rightarrow r = 0{,}106\ m$$

Chapter 4- Finite Element Analysis using ANSYS

4.1 The Finite Element Method

Differential equations that were developed back in the 17th and 18th century are used to mathematically describe the physical behaviors of elements. Analytical and numerical approaches can both be used to solve differential equations. While analytical solutions are acceptable for uncomplicated academic objectives, only numerical methods of approximation are worth considering when it comes to the varied and typically complex challenges relating to real-world scenarios. The variational method and finite difference method are two methods that were created to solve such complicated problems. By dividing any given structure into a grid, the finite difference approach provides an approximation of the solution to a differential equation. This strategy has not been widely embraced.

On the other hand, the variational methods are based on a set of approximating functions, which in turn consist of sets of unknown parameters determined by a minimization principle. This converts the problem of the differential equation into a collection of simultaneous algebraic equations for some given unknown parameters. The function used and the quantity of unknown parameters affect the accuracy of the approximation.

One such numerical method is the finite element method, which stands out due to the element-based selection of the functions and the fact that the free parameters are physically comprehensible variables that are located at the intersections (nodes) of the domains (elements); these variables could be displacements or temperatures, for instance.

Because it is designed for computers, the finite element method has achieved widespread recognition as a computational technique. This increases its potential. Simpler functions can be used, and complex geometry can be mapped, thanks to the simulation models' division into various domains or “elements".[13]

The fundamental principles of the finite element method are quite simple and straightforward. The first stage in the finite element solution is a process called discretization, in which the domain is divided into elements. The distribution of the elements that comes after is called the mesh, then the points at which the elements are connected are called joints. *Figure 4.1* [15] represents a finite element mesh of a gear tooth, where the surface is divided into triangular elements with the nodes at the corners where two or more elements are connected. [14]

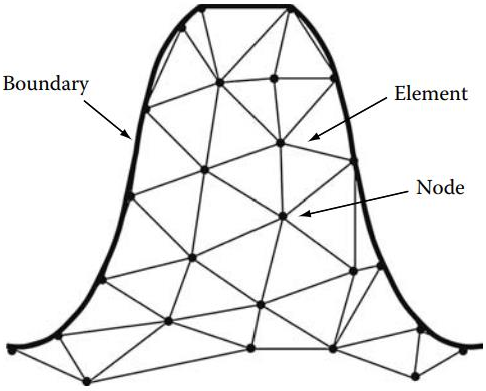

Figure 4.1 Finite element mesh of a gear tooth

After the discretization process, the predominant equations for each element must be established, and relevant material properties should be available. The equations of the elements are then compiled to attain the global equation for the mesh, the equation that describes the behavior of the body as a unity.

The global governing equation is:

$$\{R\} = [K]\{d\}$$

Where:

$[K]$ is the stiffness matrix, which connects the forces to the displacements at the nodes.

$\{d\}$ is the nodal degree-of-freedom, the displacements for structural analysis, temperatures for thermal analysis.

$\{R\}$ is the nodal external force, forces for structural analysis, heat flux for thermal analysis.

However, the element equation $\{r\} = [K]\{d\}$ should be separately generated for each element and then all elements' equations should be assembled. In addition, the boundary conditions should be introduced in the global equation.

The elements equations are of great complexity especially for a composite structure like a cable-stayed bridge. It is however important to show two examples of the element equations for the elements used in the thesis.

The element equation for the bar element is:

$$\begin{Bmatrix} r_1 \\ r_2 \end{Bmatrix} = \begin{bmatrix} E/AL & -E/AL \\ -E/AL & E/AL \end{bmatrix} \begin{Bmatrix} d_{1x} \\ d_{2x} \end{Bmatrix}$$

And the element equation for the beam element subjected to nodal forces is:

$$\begin{Bmatrix} f_1 \\ m_1 \\ f_2 \\ m_2 \end{Bmatrix} = \frac{EI}{L^3} \begin{bmatrix} 12 & 6L & -12 & 6L \\ 6L & 4L^2 & -6L & 2L^2 \\ -12 & -6L & 12 & -6L \\ 6L & 2L^2 & -6L & 4L^2 \end{bmatrix} \begin{Bmatrix} u_1 \\ \vartheta_1 \\ u_2 \\ \vartheta_2 \end{Bmatrix} - \begin{Bmatrix} -F_1 \\ -M_1 \\ -F_2 \\ M_2 \end{Bmatrix}$$

Where:

E is Young's modulus, property of the material.

A is the cross-section area of the element.

I is the moment of inertia.

L is the length of the element.

And the nomenclature of the nodal parameters of the beam element are shown in *Figure4.2* [14].

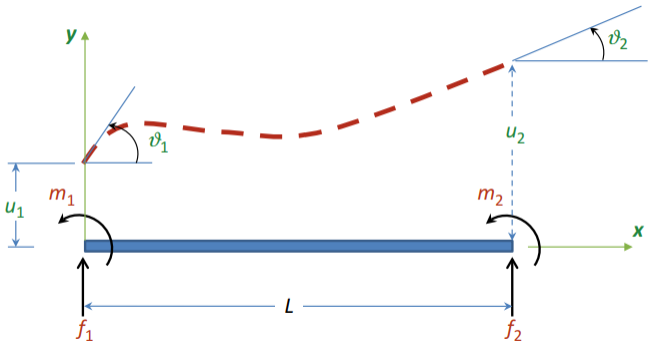

Figure 4.2 Nomenclature of the nodal parameters of the beam element subject to nodal forces

It is worth pointing that the bar elements have two degrees of freedom, whereas the beam elements have four degrees of freedom. Therefore, the 2x2 matrix for the bar and the 4x4 matrix for the beam. Beams subjected to other kinds of forces, such as uniform loadings or arbitrary varying loadings, will have more complicated element equations. When forming the global governing equation of a multi element project, the matrices turn to be of an incomprehensible size for a manual solution.

These matrices could also be put in MATLAB environment with the appropriate code, and the modeling could then be carried out. CALFEM (Computer Aided Learning of the Finite Element Method) is an interactive computational toolbox that uses the widely used mathematics program MATLAB to assist in teaching the FEM. [14]

The finite element method facilitates analyzing problems with complex geometry, studying and analyzing structures with multiple loads (pressure, thermal loadings, etc.) and solving a wide spectrum of engineering problems (structural, thermal, fluid mechanics, aerodynamics, etc.) and its almost unlimited applications in a variety of domains such as biotechnology and biomedical engineering, where it is used in the latter to simulate nonhomogeneous bone structures, modelling the nonlinear behavior of soft tissues, simulation of joints, dental and other types of implants.[16]

4.2 ANSYS Workbench

In 1963, Dr. John Swanson used computer codes to model, analyze and predict stress and displacement resulting from thermal and pressure loads in a nuclear reactor. He was working on developing and combining codes to create a comprehensive 3D analysis tool that would save time and money, i.e., a multi-purpose Finite Element Analysis FEM code.

By the end of 1970, the first version of ANSYS was coded and then released shortly after. The later versions were strongly related to the revolutionary developments and milestones in Operating Systems. With Windows 95 release, it was a huge step for using PCs as workstations by engineers, and later came the GUI (Graphical User Interface) and then CAD tools (Computer Aided Design) and all that was gradually and appropriately integrated into ANSYS though it's versions. [17]

The prominent and comprehensive functions of today's ANSYS Workbench allow data integration across engineering simulations to efficiently generate more precise models by organizing all the simulation data in one place, i.e., integrating multiple analysis functions/processes in one unified interface. That saves time and creates models of higher reliability. [18]

4.3 Meshing

Meshing is a technique for creating a 2D or 3D grid over a geometry so that it can be discretized and examined via simulation. The intricacy of geometry is then used to define the grids. Since Finite Differences relies on the adjacent cells and nodes to give an approximate representation of the behavior of the variables, they have historically been connected to rectangular and Cartesian grids [19][20]. A mesh is regarded structured, and otherwise unstructured, if the connectivity of this mesh is of the finite difference type [21]. Unstructured meshes were however made possible by the Finite Element Method (FEM), which supported mixed sorts of mesh cells. The studies carried out from the latter half of the 19th century to the first decade of the 20th century are the earliest known examples of variational formulations being applied to numerical issues.

The discretization of the equations and the problem domain are the first steps in solving a set of partial differential equations (PDE) numerically. This is when the initial continuous problem, i.e., the PDE model, is substituted by a discrete problem which, thanks to the capability of the existing computers, can be computed. The precision of the approximate solution to the discrete problem is dependent on the numerous choices that were taken during the numerical procedure. As was previously stated, it is impossible to solve the full problem domain at once, but it is possible to solve the problem domain in smaller, more manageable chunks.[19][20][21]

The process of discretizing equations is similar to techniques like the Finite Element Method, which transforms equations in continuous form into a set of algebraic difference equations. A set of discrete cells and, consequently, points or nodes that cover the continuous problem domain are produced by the domain discretization procedure.[19][20]

Mesh creation encompasses a variety of topics and domains, specifically for numerical simulation applications. These involve extensive understanding of what is commonly referred to as computer science, classical geometry, so-called computational geometry, and numerical simulation related to engineering issues. It can truly be calculated because of the power of computers that are now in use.

This categorization of disciplines that can interact while creating meshes for numerical simulations demonstrates very clearly why this subject is not that simple. People with backgrounds in geometrics, computational geometry, or mathematics may not all share the same ideas about what a mesh should be, and as a result, may not all agree on the best way to design a mesh.

Meshes are primarily interesting from a strictly geometrical perspective because of the characteristics that a particular geometrical object, like a triangle, possesses. Aspect ratios, angle measurements, orthogonality properties, affine properties, and numerous associated

constructions (centroids, circumcircles, incircles, characteristic points, intersections, etc.) have all been investigated in this context regarding the properties of such an element.

From a computational geometry perspective, the main attention is given to the theoretical aspects of triangulation methods, including a detailed examination of the relevant complexity. These methods have drawn a lot of attention in this regard since they have good theoretical underpinnings and produce thought-provoking theoretical findings. Nevertheless, triangulation methods must sometimes be tweaked or adjusted in order to be used for general meshing applications. Mesh creation from a numerical perspective, on the other hand, tends to reduce the mesh to a unity of finite, basic shaped elements with a size that approaches zero.

The challenge is therefore to create techniques that can create a computer-generated mesh that complies with the requirements of both numerical and more generally engineering approaches. One the one hand, when considered in terms of practical computer implementation, theoretical results about triangulation methods via computational geometry, may not be very realistic. On the other hand, engineering specifications may slightly deviate from what is implied or required by the theory.[21]

In conclusion, a mesh could be defined as a network made up of connected points and cells. The topology and geometry of this network can take many different forms. Meshes are frequently referred to as grids, and this is typically because of the inherent organization of the mesh or when it is used to solve Finite Differences problems. Each node or cell of the mesh, depending on which the equations were discretized over, will have a local solution of the equations. [21]

When referring to 3D models in ANSYS, there are two types of meshing depending on the element geometric nature: [18]

Tetrahedral element meshing (tet)

Hexahedral element meshing (hex)

Where tetrahedral and hexahedral are solid figures that have four and six faces respectively, as shown in *Figure 4.3* and *Figure 4.4*.[22]

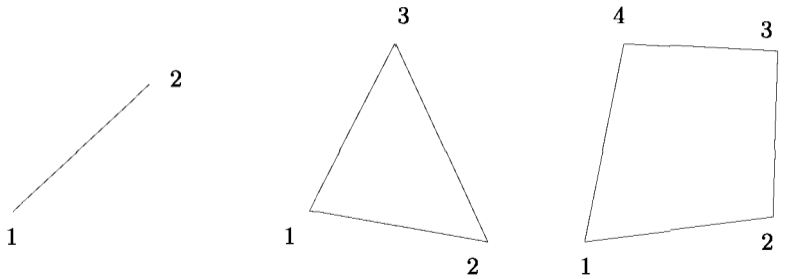

Figure 4.3 Line, Triangle and Quadrilateral (2D area elements)

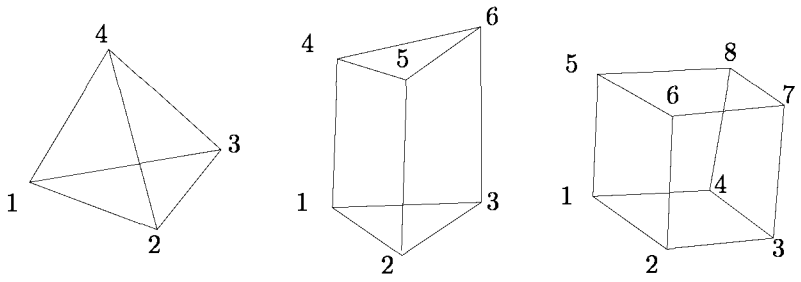

Figure 4.4 Tetrahedron, Pentahedron and Hexahedron (3D volume elements)

4.4 Simulation

The simulation of the bridge in ANSYS Workbench includes 2 types of elements:

Link/Truss (also called bars) for the stayed cables, and beams for the bridge beam, towers, and the bridge plate. The choices of the types of the elements were based on the results analysis type that were chosen for this thesis, i.e., static analysis of forces where the dynamic forces affecting cables were not taken into consideration and thus not to be calculated.

The bridge plate was simulated as a beam element as it will be later meshed and set in contact with the girders and the bridge beam. The dimensions of the bridge plate were the same as in the original bridge.

The boundary conditions were chosen taking into consideration the design of the bridge and to avoid the indeterminacy of degrees of freedom. Boundary conditions are positioned as shown in *Figure 4.5* and are selected as follows:

Points **E** and **F** (the bases of the towers) are fixed supports.

Point **G** () is a fixed support.

Point **B** () is a simple support.

The forces applied on the bridge are the ones resulted from calculating wind loads and traffic loads. Yet, the best way to simulate those forces in ANSYS workbench was to use the line pressure forces and apply it on the plate for the live loads and on two of the sides of the bridge beam as in *Figure 4.5*.

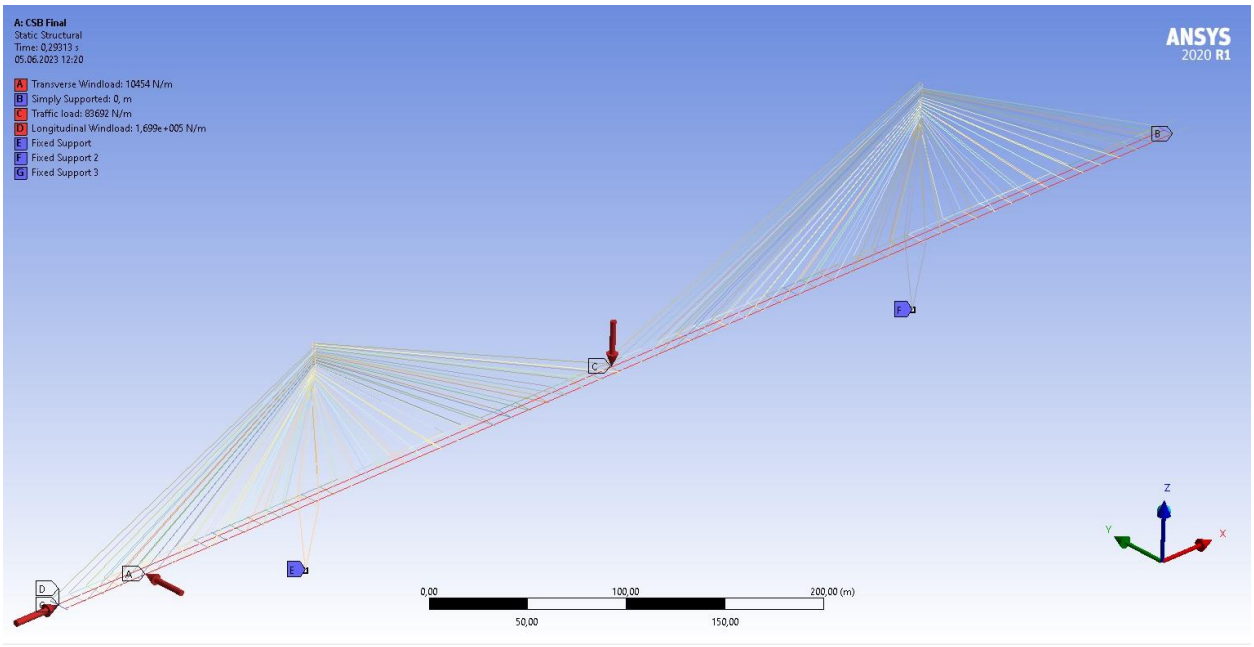

Figure 4.5 Static structural view of the bridge with the supports and forces applied on elements of the bridge

It should be noted that the Y and X axes in the calculations of the wind loads and here in the simulation are inverted. That makes clearly no difference for the results but it must be nevertheless mentioned.

Chapter 5- Results, Discussion and Conclusion

5.1 Results

For the purpose of this project and static analysis criteria, the five aspects that will be examined are:

1. Deformed shape for the whole structure: to understand the response of the structure to the applied loads, assess the behavior and verify the overall structural performance of the structure.
2. Von Mises stress distribution: Also known as the equivalent stress, which measures the combined stress state in a material. The single value that it provides is often used to assess the strength and failure criteria of materials when subjected to complex loadings.
3. Bending moment distribution.
4. Shear force distribution.
5. Axial force distribution.

To assess the magnitude and distribution of the bending, shear, and axial forces respectively within the structure.

Figures 5.1 to 5.7 Below show the results from ANSYS Workbench.

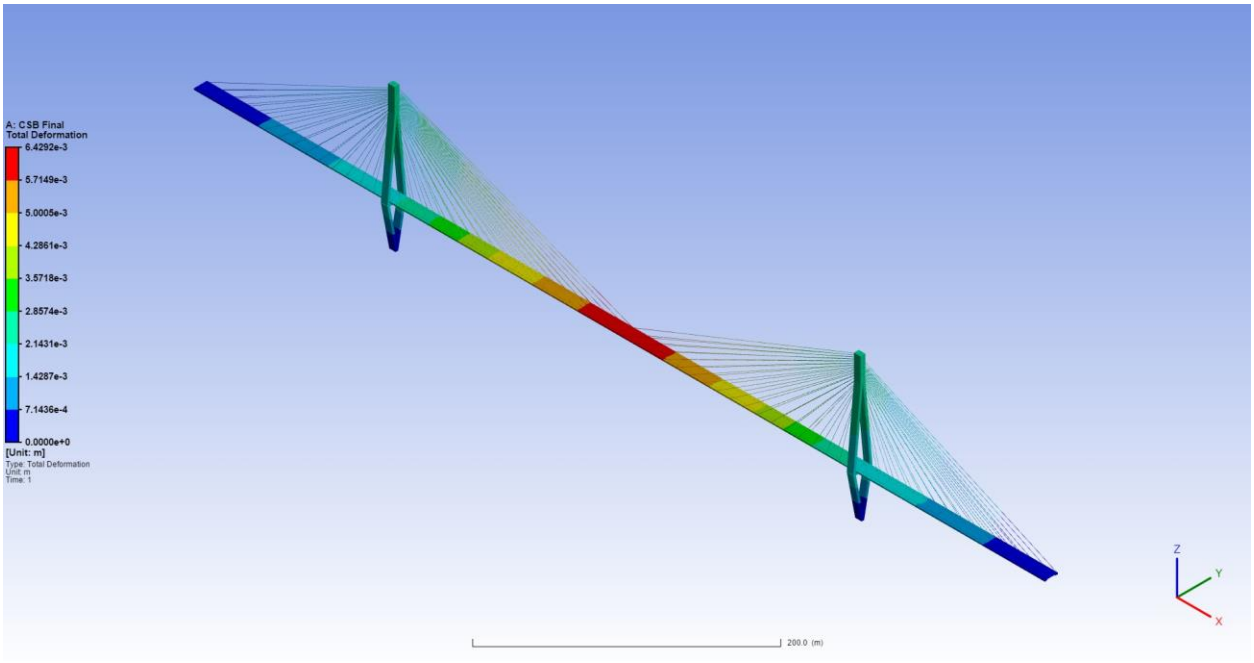

Figure 5.1 Total deformation of the whole structure

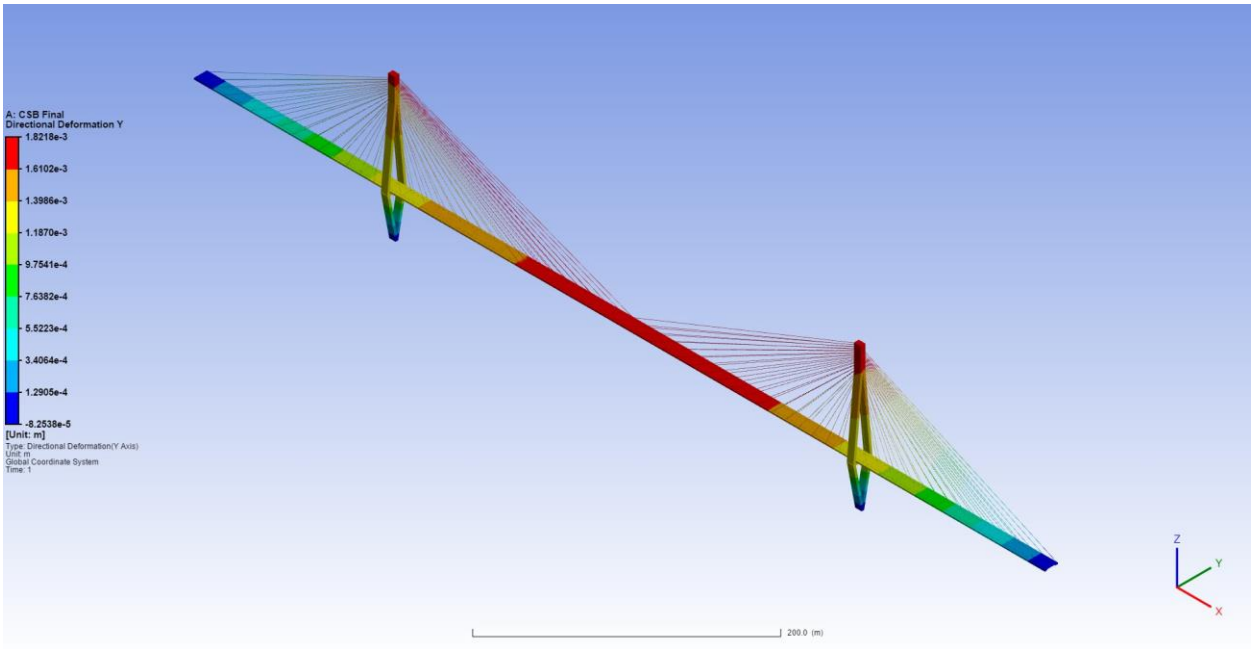

Figure 5.2 Directional deformation of the structure in Y direction

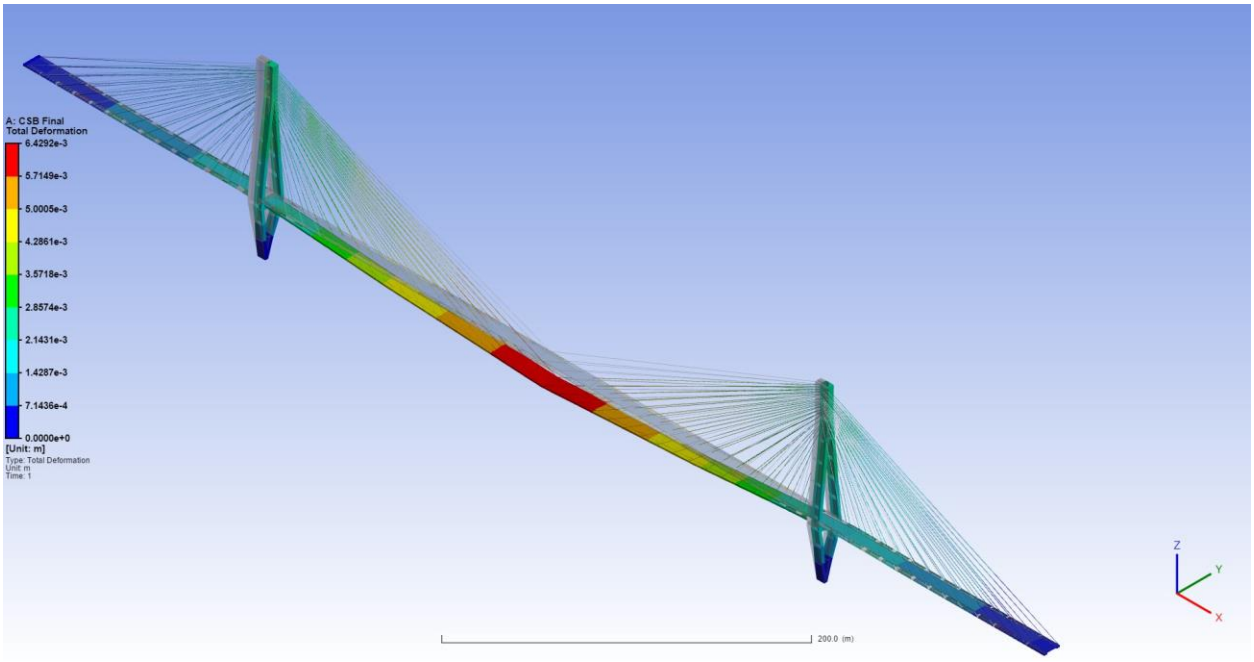

Figure 5.3 Exaggerated model for the total deformation of the whole structure

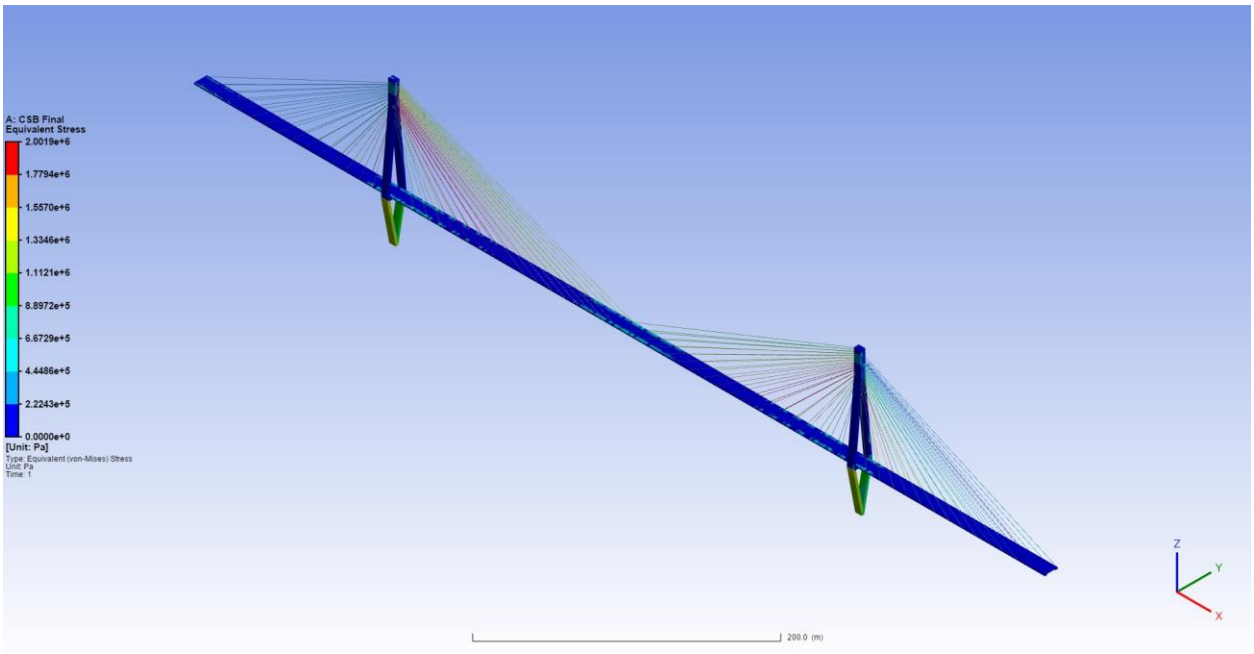

Figure 5.4 Von Mises Stress (Equivalent Stress)

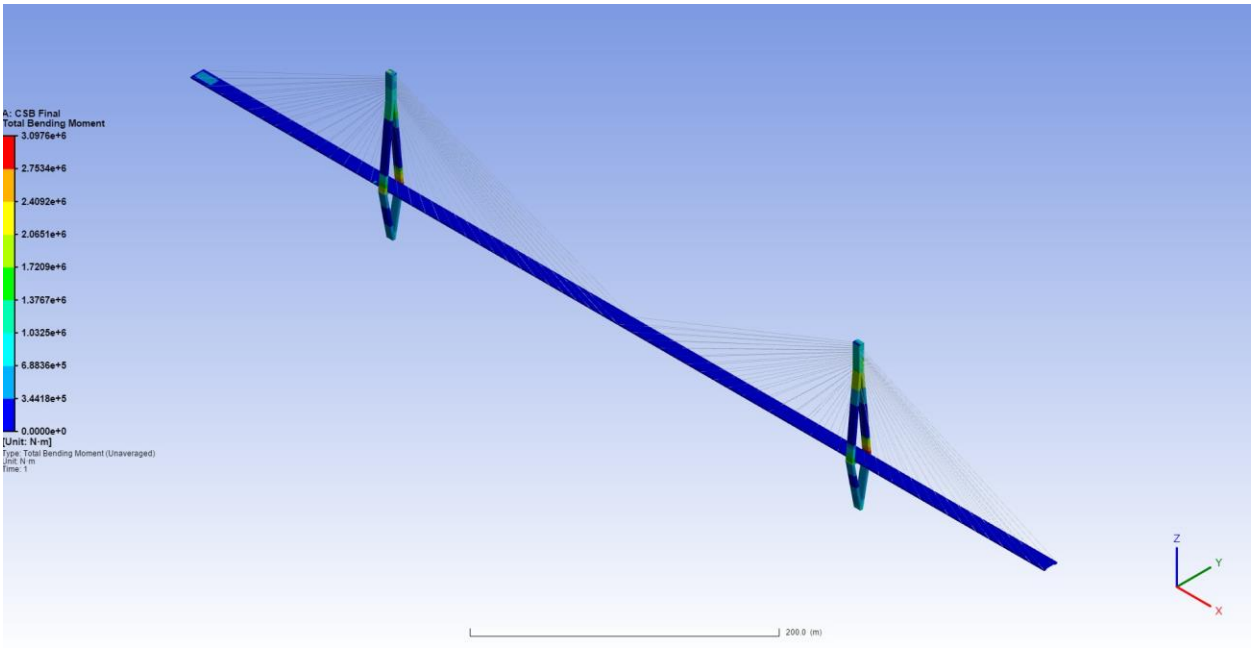

Figure 5.5 Total bending moment

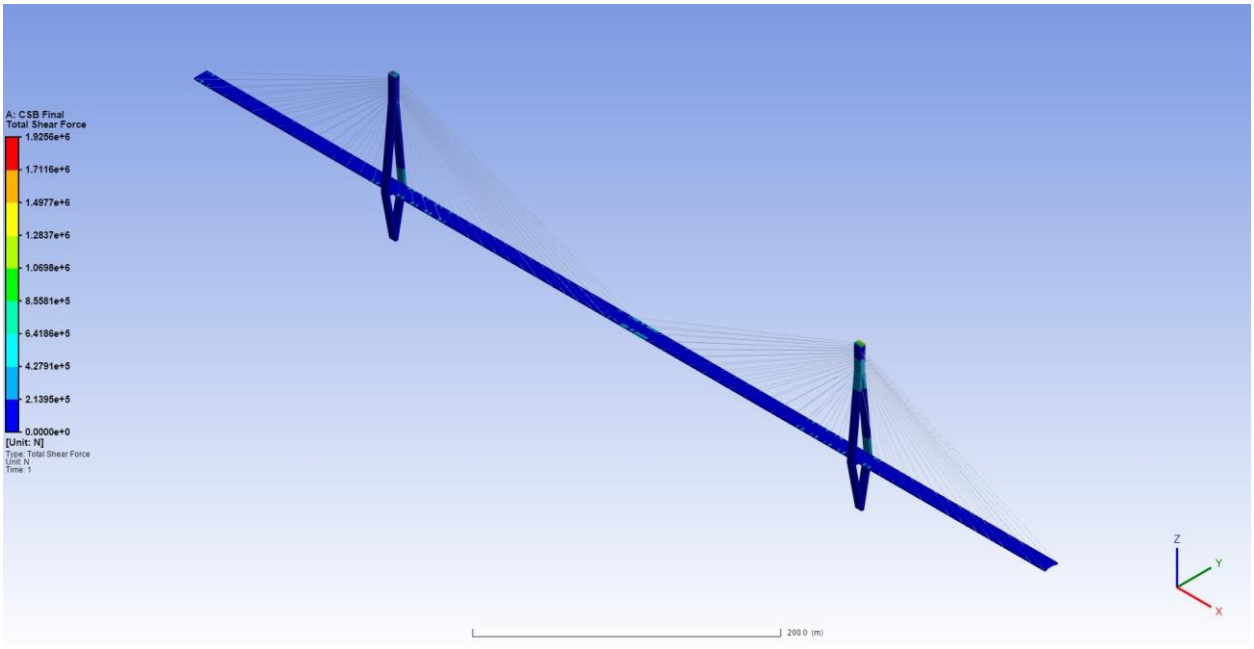

Figure 5.6 Total shear force

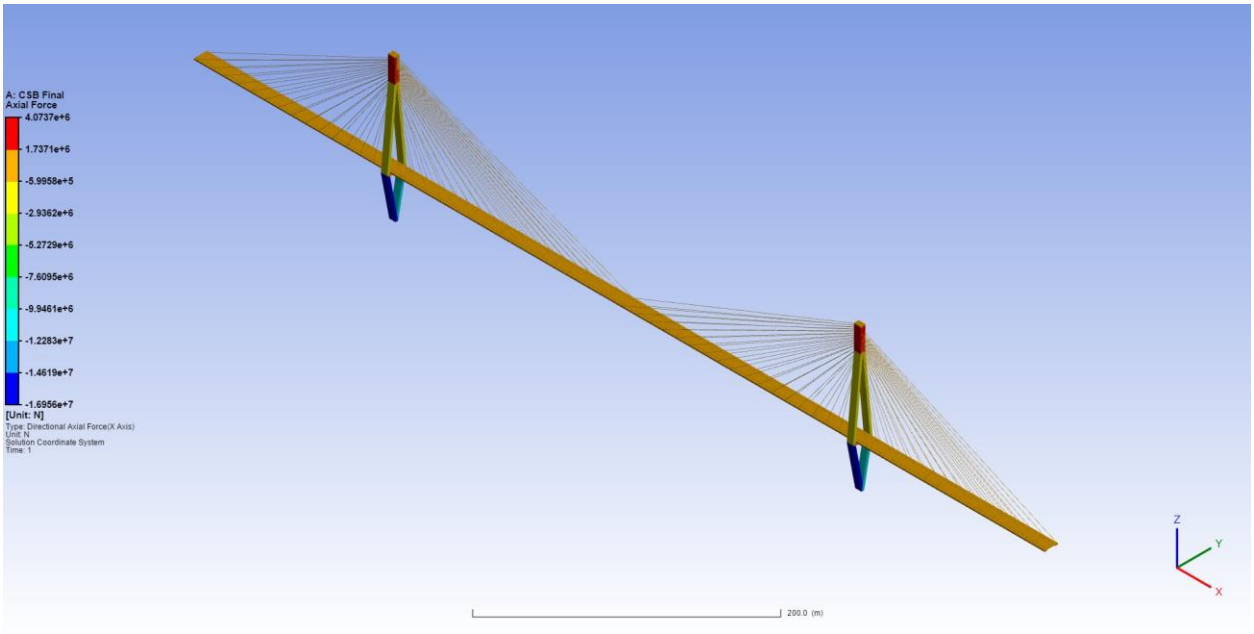

Figure 5.7 Axial force

Starting the count of cables and towers at point (0,0,0) (at the far end of the figures), the results could be summed up as follows:

- The total deformation of the structure reaches a maximum of $6{,}43 * 10^{-3}m$ in the middle of the bridge at the furthest area from the towers, in addition to the part of the cables connected to the bridge deck at the same area, and at minimum of 0 on both edges and at the bases of the towers due to the constraints at these points.
  Directional deformation in the positive Y direction is at $1{,}8 * 10^{-3}m$ due to the transverse wind loads.
  Figure 5.3 shows the exaggerated deformation of the bridge -with the original position in the view- which happens in negative Z and positive Y directions.
- The Von Mises stress reaches a maximum of $2 * 10^{6}Pa$ on some of the cables (Specifically 13, 19-23, 41-43) and the ones symmetrical to them from the other side.
- The bending moment reaches a maximum of $3{,}1 * 10^{6}Pa$ at the two inner points of the towers where the bridge deck lays on.
- Shear force reaches a maximum of $1{,}925 * 10^{6}Pa$ at the top of the first tower.
- Axial force reaches a maximum of $4 * 10^{6}\ Pa$ at the higher parts of the towers.

5.2 Discussion and Conclusion

All the maximum values of Von Mises stress, bending moment, axial and shear force are in the limits, i.e., smaller than the maximum tensile yield strength (steel) and ultimate strength (concrete) of the construction materials of the bridge, which indicates the maximum stress a material can sustain without permanent deformation., as could be noticed from *Table 1.5*. [23][24]

The values in the table are similar to the engineering data of the materials used in ANSYS. The engineering data is provided in the Appendix.

Material	Tensile Yield strength [MPa]	Tensile Ultimate strength [MPa]
B65 Concrete	65	5
Structural Steel	240	360

Table 5.1 Tensile Yield and Ultimate Strength for B65 Concrete and Structural Steel

The total deformation of the structure is very small due to the large number of cables at the maximum cross section with regard to not calculating the wind loads on the towers and on the bridge deck on the Z axis.

The shear force and bending moment are mostly zero and in the minimum for the most parts of the structure because of the large number of cables regarding the applied forces, in addition to the chosen boundary conditions.

Overall, the limitations of the static analysis have led to the small deformation and generally damping of the bending moment and shear forces. When wind loads on the Z axis, wind loads on the towers, and the oscillation effects on the cables are considered, the bending moment and shear force distribution would have higher values and greater distribution. The total deformation would also have a larger value.

Regarding the forces applied on the structure and the main goal of this project, the bridge is statically stable and the criteria for the static analysis of a stable design are satisfied, and the Finite Element Analysis of this cable-stayed bridge has resulted in a statically stabled simulated structure.

References

[1] Cable-Stayed Bridges 40 Years of Experience Worldwide. Svensson, Holger, 2012

[2] Encyclopedia Britannica

[3] https://www.roadtraffic-technology.com/features/top-ten-longest-cable-stayed-bridges-in-the-world/

[4] Construction Stage Analysis of Cable-Stayed Bridges. Marko Justus Grabow, Technical University of Hamburg Harburg, Germany 2004.

[5] Static and Dynamic Analyses of a Long-Span Cable-Stayed Bridge with corroded cables. Xiang Yang 2018. University of Ottawa, Canada 2018.

[6] Wind effects on Cable-supported bridges, You-Lin Xu, The Hong Kong Polytechnic University, Hong Kong, P. R. China. 2013 John Wiley & Sons Singapore Pte. Ltd.

[7] Structural Analysis. Russell C. Hibbeler 9th Edition. Published by Pearson Prentice Hall

[8] Wind loads on bridges, M. Sajad Mohammadi Rishiraj Mukherjee. Master Thesis 385, 2013. Royal Institute of Technology KTH, Stockholm, Sweden

[9] EN 1991-1-4:2005+A 1. Eurocode 1: Actions on structures - Part 1-4: General actions - Wind actions.

[10] EC1-EN-1991-1-2-Traffic loads on road bridges

[11] NS EN 1991-2 Traffic loads

[12] https://www.itf-oecd.org/sites/default/files/docs/dimensions-2019.pdf

[13] The origins of the finite element method (cadfem.net)

[14] Essentials of the finite element method. Dimitrios G. Pavlou. University of Stavanger, Norway 2015. Elsevier Inc.

[15] Finite Element Simulations Using ANSYS. Alawadhi, Esam M. 2nd Edition. Kuwait University, Safat. CRC Press 2016.

[16] FEM of biomedical engineering applications, Z.Yang, CRC Press 2019.

[17] Finite Element Simulations with ANSYS Workbench. Huei-Huang Lee, 2020. Cheng Kung University, Taiwan. SDC Publications.

[18] https://www.ansys.com/

[19] What is a Mesh? | SimWiki Documentation | SimScale

[20] The Fundamentals of FEA Meshing for Structural Analysis (ansys.com)

[21] Thomée, V., “From finite differences to finite elements: A short history of numerical analysis of partial differential equations”, 2001

[22] Mesh Generation Application to Finite Elements, Second Edition. Pascal Jean Frey, Paul Louis George. Wiley.

[23] ((2004). NS-EN 1991-1-1:2002+NA:2008 -Eurokode 2: Prosjektering av betongkonstruksjoner -Del 1-1: Allmenne regler og regler for bygninger. Standard Norge, 1326 Lysaker.)

[24] Structural Steel - an overview | ScienceDirect Topics

Appendix ANSYS Steps and Procedure

The goal of this appendix is to provide an overview of the work steps and the difficulties that were encountered to better present the efforts that were put into the simulation part of this thesis, and to highlight some of the problems that might save other students quite some time especially while using ANSYS Workbench for a structural project, because the practical resources available online (YouTube videos and courses) are mostly for mechanical, thermal and machine design. That is not to say that those resources are not helpful; however, the different goals and methodology of a structural project could render it unusable when it comes to some crucial details.

The stages of the project were quite straightforward. Starting with selecting the engineering data for the materials used in the bridge, then sketching the geometry of the bridge and assigning the elements each to its appropriate cross section.

After the geometry was completed, the modelling of the project starts with assigning the materials and the types of elements for the simulation and meshing. When the meshing was processed by the software, setting up the boundary conditions and the forces applied on the bridge was carried out and finally solution information was put in and solved by the program.

The workflow was not free of hiccups and obstacles though, and a brief description of the major issues is provided with the necessary figures.

- Engineering Data

Starting with the material selection for the project is one of the first steps to be taken. For this project, the materials needed were already available with the appropriate properties, as shown in the figures below, when compared with the real materials used to build the actual bridge.

In case the materials were available with different properties, the values could easily be changed. If special materials were to be used and do not exist in the software, it could be manually added to the engineering data and plenty of YouTube tutorials are available regarding this. However, new added materials would empirically make the solution prone to errors and/or error messages.

Properties of Outline Row 3: Concrete

	A	B	C	D	E
1	Property	Value	Unit		
2	Material Field Variables	Table			
3	Density	2300	kg m^-3		
4	Isotropic Secant Coefficient of Thermal Expansion				
6	Isotropic Elasticity				
12	Tensile Yield Strength	0	Pa		
13	Compressive Yield Strength	0	Pa		
14	Tensile Ultimate Strength	5E+06	Pa		
15	Compressive Ultimate Strength	4,1E+07	Pa		

Properties of Outline Row 4: Structural Steel

	A	B	C	D	E
1	Property	Value	Unit		
2	Material Field Variables	Table			
3	Density	7850	kg m^-3		
4	Isotropic Secant Coefficient of Thermal Expansion				
6	Isotropic Elasticity				
12	Strain-Life Parameters				
20	S-N Curve	Tabular			
24	Tensile Yield Strength	2,5E+08	Pa		
25	Compressive Yield Strength	2,5E+08	Pa		
26	Tensile Ultimate Strength	4,6E+08	Pa		
27	Compressive Ultimate Strength	0	Pa		

- Limited Number of Elements

First and foremost, the simple but hugely obstructing issue that was encountered in the beginning was the number of the elements (parts/bodies in the software terminology) that the program was allowing. After much research it turned out to be a simple step from Design Modeler window:

Units >> Large Model Support >> On

However, the program will not allow this change in the middle of the project and would require this simple change to be made at the very beginning of the work. Therefore, the sketching and geometry part had to be restarted in a new file.

- Mesh Size

When changing the mesh size to a smaller size than the default one, the software and/or the computer might very well freeze and stop working especially for a project of this size and number of elements. The interrupt function was not of a big help, and neither was the END TASK function of the Windows operating system, and that is because when closing and reopening the software, the mesh would start again from the interruption point and would continue to be frozen. The simple solution for this problem was to add a new **Static Structure System** and transfer the engineering and geometry data to it. However, the model cannot be transferred and should be redone.

The figures below show the simple 3 step solution. The **Static Structure System B** is then ready to be further modelled.

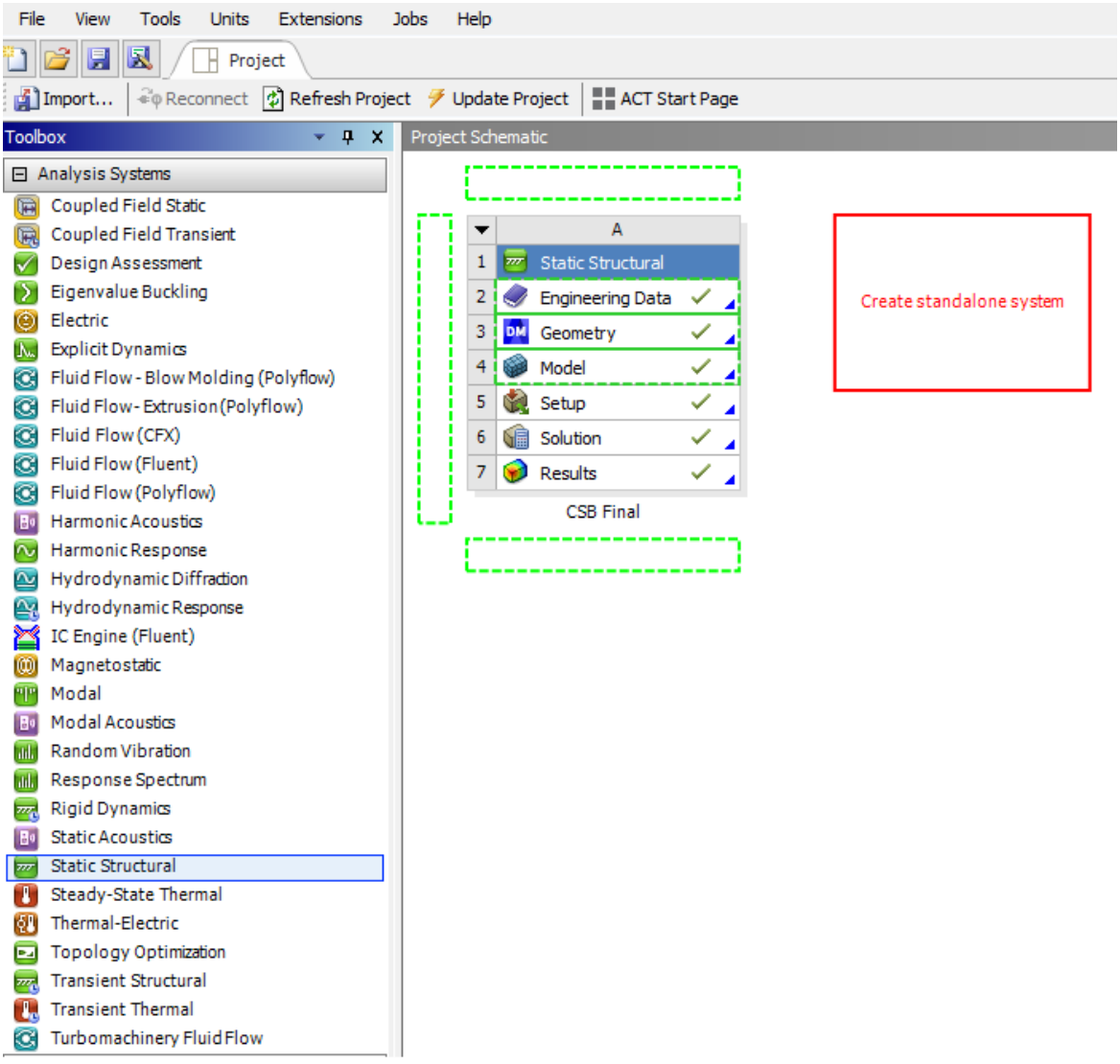

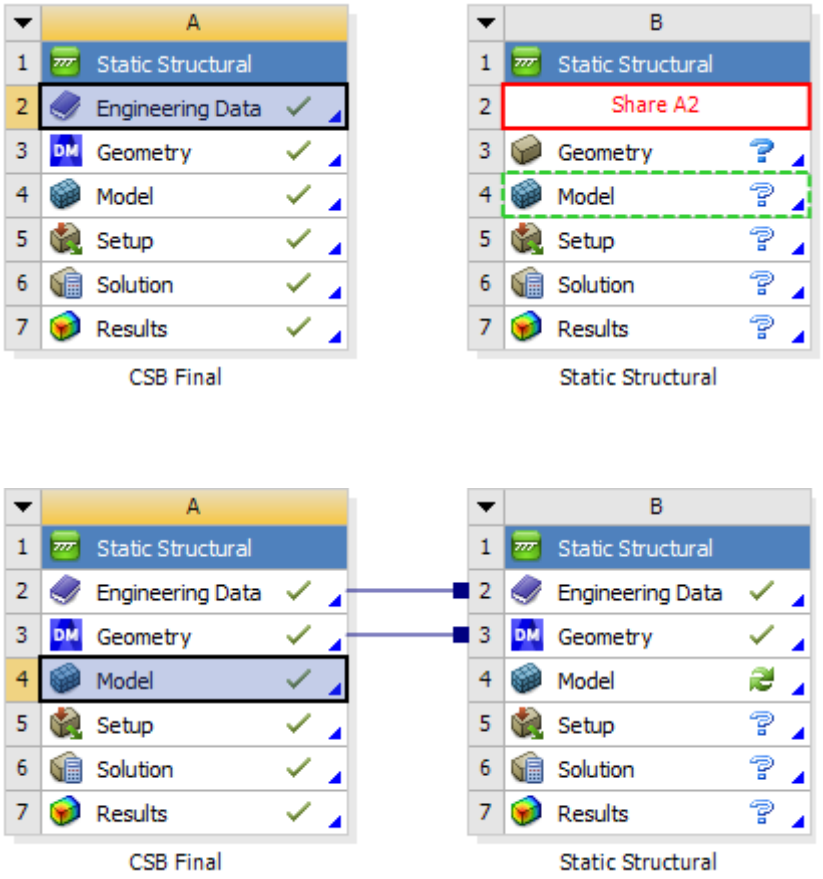

It could be easily noticed that the two towers are of different colors. That is because after placing the points on the one tower to draw the cables from, the points turned suddenly inactive, and the function **Line from Point** was not able to detect them. This was unexpected and it required drawing another tower from the beginning and placing the points again. However, the old tower needed to be suppressed using the function **Suppress Body** in order to not have two towers on top of each other after the **Mirroring**. This resulted in a mirrored tower with a different color.

- Mirroring

The mirror function was used after drawing one of the towers and connecting the cables on it. It was discovered by try and error that it is of a great benefit to create new planes with defined translation from the original XYZ planes and draw on them because not only it saves much more time than making body transformations, but also allows to make changes to the figures/elements without any problems. The program would not allow any position or dimension editing (and clearly no removing) on any element that is used as a reference for any

kind of body transformation, and this makes any correction or edit complicated and sometimes not possible without redoing the whole geometry (as it happened during this project) or at least prats of it. That could be easily avoided by drawing in new planes. The same goes for using new planes for the mirroring process since it is much more precise to do this procedure in reference to a plan.

- Edge Sizing for the cables (bar/link/truss elements)

One of the useful options for Edge Sizing control is determining how the mesh is spread throughout the length of the edge for the element being meshed. What was needed to be done here is to make the cables sized edge to edge with one division, i.e., meshing each one of them as a single size element.

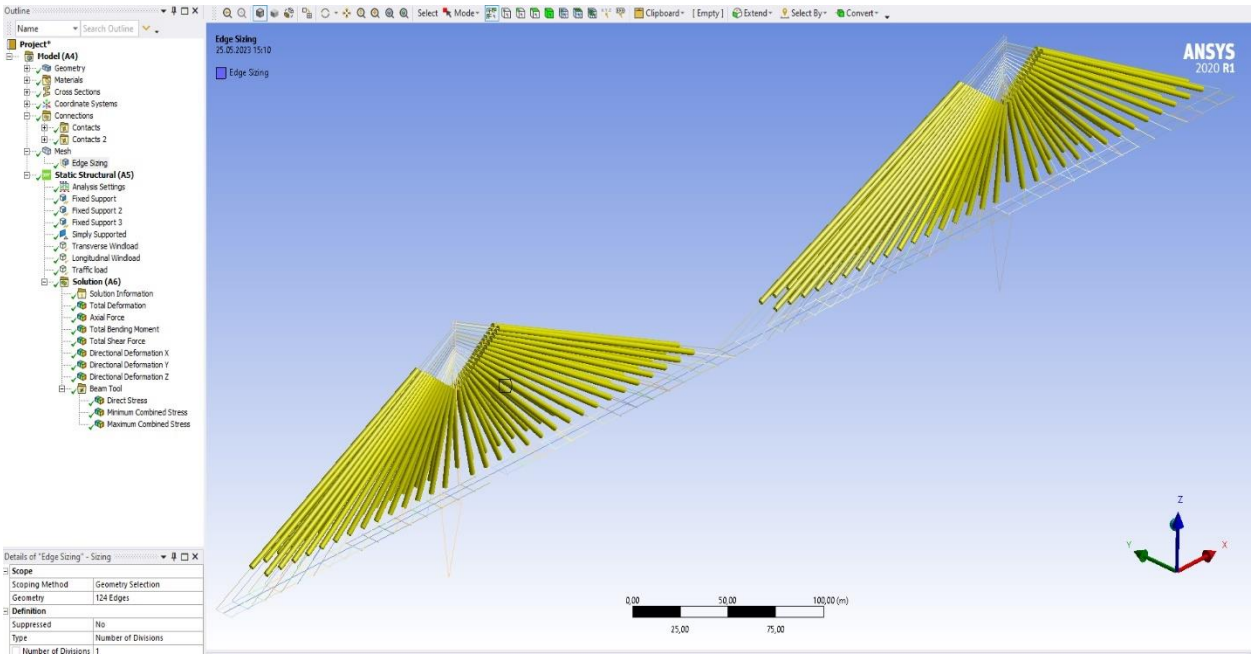

- Contact Regions

The contact regions had to be done manually between each of the cables and the bridge deck and between the bridge deck and the bridge plate. This is because the automatic contact region function was not sufficient. It was found when taking the exaggerated deformation simulator that the elements of the bridge deck were disintegrating and thus there was something wrong with the contacts between the elements.

The figures show how to start the **Manual Contact Region** function, and how the program then processes it and creates contact regions between the elements. This bridge ended up with 1994 contact regions.

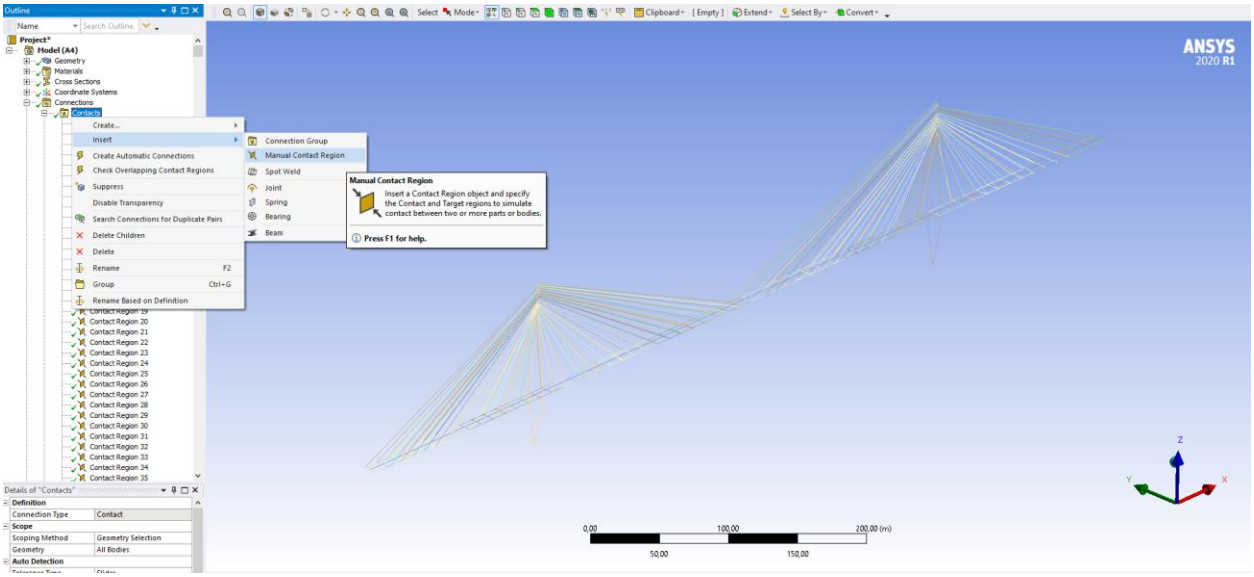

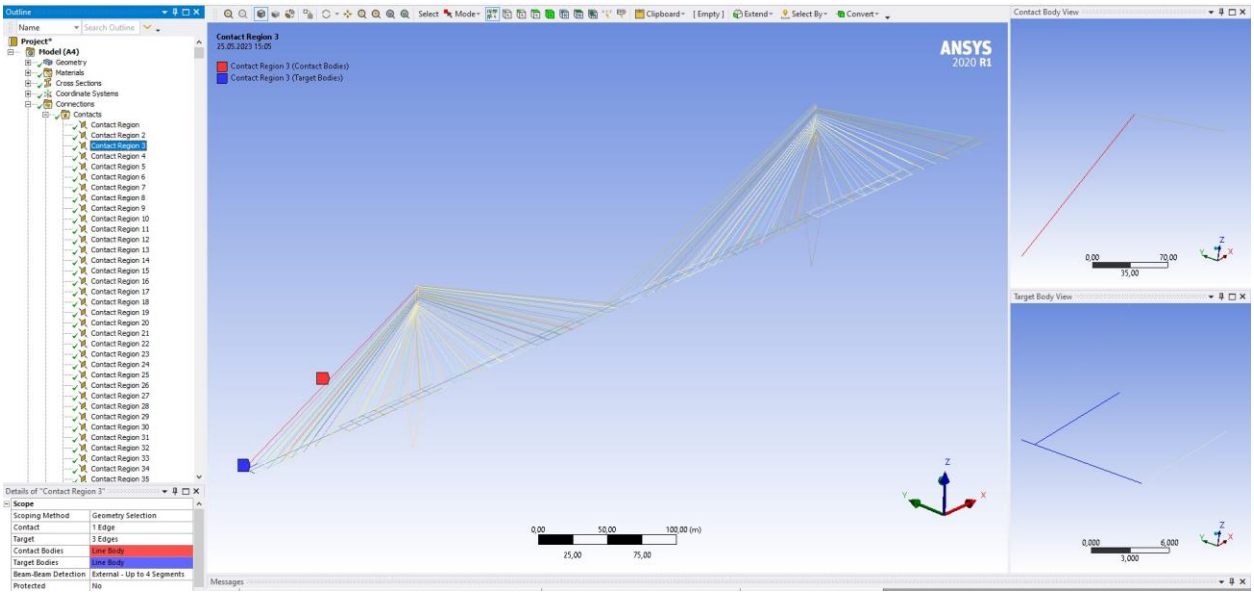

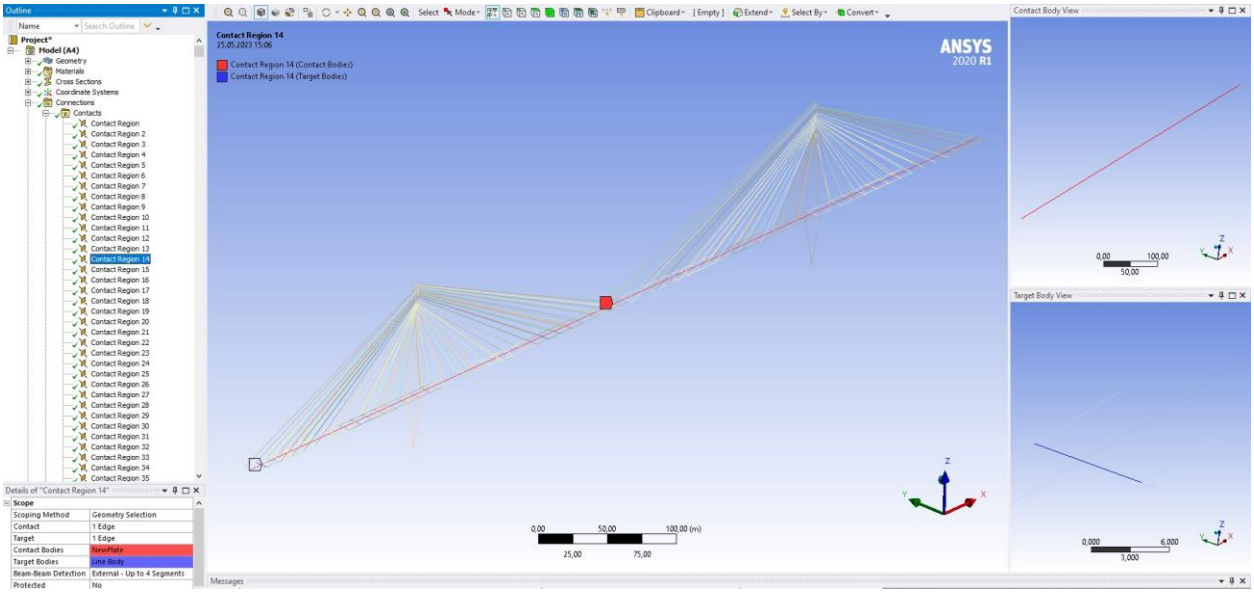

- Solution Information

After finishing all the steps of the meshing and running the solution, it is of a great importance to pay attention to the warnings that will come up in the solution information, and carefully read what details are mentioned and whether there should be any further actions taken.

The last problem that was encountered during this project was not being able to insert a Von Mises solution option in the solution information list. The solution for that was simply pointed out in the first warning in the solution information list as shown in the figure below.

“No stress/strain results are found on beams. Please set the Beam Section Results to Yes”

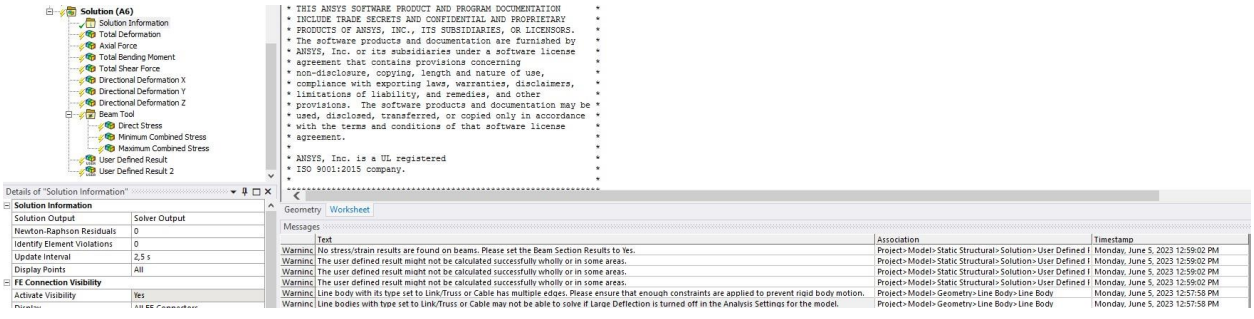

As shown in the figure below, changing the Beam Section Results to Yes and running the solution again would solve that problem.

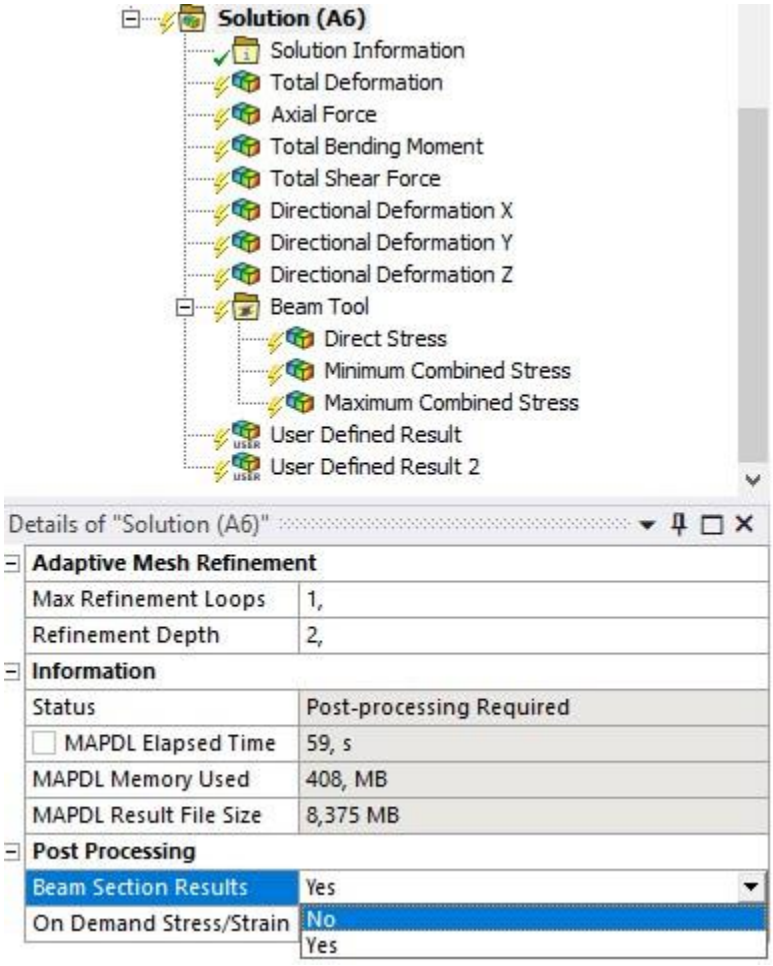

It is worth pointing out that in some cases/versions of the software, the Von Mises might not appear in the direct options in the solution menu. That is simply solved by adding a **User Defined Result** and then manually writing the expression for the Von Mises solution in the expression field. The expression is given as:

seqv*(sx+sy+sz+1e-6)/abs(sx+sy+sz+1e-6)

It is necessary to state that if the **Beam Section Result** is not turned to Yes, writing this expression in a **User Defined Solution** would give a zero result as shown in the figure below.

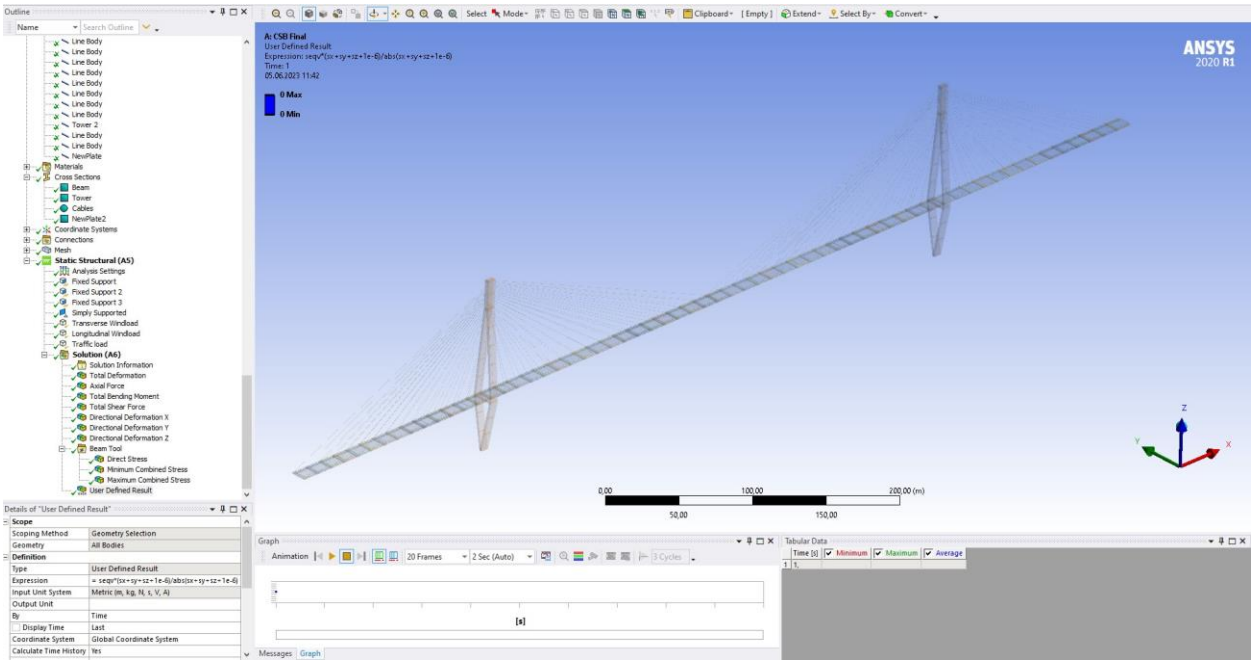

Finally, it is worth mentioning that the figures for the results were obtained by exporting AVZ files, as shown in the figure below, and then taking screenshots of the files.

Exporting AVZ files is an effective and practical way to interactively present the results of a project in high quality 3D animated file without having to run ANSYS software, which could be heavy for the PC and quite time consuming often. Installation of the ANSYS software on the device is however required and the AVZ files could not be used without it.